ELSEVIER

Contents lists available at ScienceDirect

International Journal for Parasitology

journal homepage: www.elsevier.com/locate/ijpara



Co-infecting *Haemoproteus* species (Haemosporida, Apicomplexa) show different host tissue tropism during exo-erythrocytic development in *Fringilla coelebs* (Fringillidae)



Tanja Himmel ^{a,*}, Josef Harl ^a, Julia Matt ^a, Nora Nedorost ^a, Madeleine Lunardi ^a, Mikas Ilgūnas ^b, Tatjana Iezhova ^b, Gediminas Valkiūnas ^b, Herbert Weissenböck ^a

ARTICLE INFO

Article history: Received 2 June 2023 Received in revised form 12 July 2023 Accepted 14 July 2023 Available online 19 August 2023

Keywords:
Avian haemosporidians
Haemoproteus
In situ hybridization
Laser microdissection
Meront
Megalomeront

ABSTRACT

Avian haemosporidians of the genera Plasmodium, Haemoproteus, and Leucocytozoon are common blood parasites in wild birds all over the world. Despite their importance as pathogens potentially compromising host fitness and health, little is known about the exo-erythrocytic development of these parasites, particularly during co-infections which predominate in wildlife. This study aimed to address this issue using Haemoproteus parasites of Fringilla coelebs, a common bird species of the Western Palearctic and host to a variety of haemosporidian parasite lineages. Blood and tissue samples of 20 F. coelebs, positive for haemosporidians by blood film microscopy, were analysed by PCR and sequencing to determine cytochrome b lineages of the parasites. Tissue sections were examined for exo-erythrocytic stages by histology and in situ hybridization applying genus-, species-, and lineage-specific probes which target the 18S rRNA of the parasites. In addition, laser microdissection of tissue stages was performed to identify parasite lineages, Combined molecular results of PCR, laser microdissection, and in situ hybridization showed a high rate of co-infections, with Haemoproteus lineages dominating. Exo-erythrocytic meronts of five Haemoproteus spp. were described for the first known time, including Haemoproteus magnus hCCF6, Haemoproteus fringillae hCCF3, Haemoproteus majoris hCCF5, Haemoproteus sp. hROF11, and Haemoproteus sp. hCCF2. Merogonic stages were observed in the vascular system, presenting a formerly unknown mode of exo-erythrocytic development in Haemoproteus parasites. Meronts and megalomeronts of these species were distinct regarding their morphology and organ distribution, indicating species-specific patterns of merogony and different host tissue tropism. New pathological aspects of haemoproteosis were reported. Furthermore, phylogenetic analysis of Haemoproteus spp. with regard to their exo-erythrocytic stages points towards separation of non-megalomeront-forming species from megalomeront-forming species, calling for further studies on exo-erythrocytic development of haemosporidian parasites to explore the phylogenetic character of this trait.

© 2023 The Author(s). Published by Elsevier Ltd on behalf of Australian Society for Parasitology. This is an open access article under the CC BY license (http://creativecommons.org/licenses/by/4.0/).

1. Introduction

Avian haemosporidian parasites of the related genera *Plasmodium*, *Haemoproteus*, and *Leucocytozoon* (order Haemosporida, Apicomplexa) are globally spread and commonly found in wild birds of most orders (Clark et al., 2014). These obligate heteroxenous blood parasites are genetically highly diverse and differ in many

ecological aspects such as vector and host specificity, prevalence, and geographic distribution (Scheuerlein and Ricklefs, 2004; Križanauskienė et al., 2006; Hellgren et al., 2009; Santiago-Alarcon et al., 2012; Clark et al., 2014; Ellis et al., 2020; Fecchio et al., 2020). Moreover, avian haemosporidians have distinct life cycles and display varying levels of pathogenicity (Atkinson et al., 1991; Valkiūnas, 2005; Palinauskas et al., 2008; Ilgūnas et al., 2019a), providing the opportunity to study host-parasite relationships and test hypotheses about their evolutionary history.

Approximately 270 species (177 Haemoproteus spp., 55 Plasmodium spp., 45 Leucocytozoon spp.) have been described so far based on morphological characters of the parasites' blood stages

a Institute of Pathology, Department for Pathobiology, University of Veterinary Medicine Vienna, Veterinaerplatz 1, 1210 Vienna, Austria

^b Nature Research Centre, Akademijos 2, 08412 Vilnius, Lithuania

^{*} Note: Nucleotide sequence data reported in this paper are available in GenBank under accession numbers <u>OR250625-OR250656</u>.

^{*} Corresponding author at: Institute of Pathology, Department for Pathobiology, University of Veterinary Medicine Vienna, Veterinaerplatz 1, 1210 Vienna, Austria. E-mail address: tanja.himmel@vetmeduni.ac.at (T. Himmel).

(Valkiūnas, 2005; Valkiūnas and Iezhova, 2018, 2022, 2023). Thanks to their easy access in the circulating blood of avian hosts, and widely applied PCR-based diagnostics, this species number has long been exceeded by an enormous count of 4839 unique lineages at this time based on a short fragment of the parasites' mitochondrial cytochrome b (*cytb*) gene (MalAvi database, Lund University, Lund, Sweden, https://130.235.244.92/Malavi/, accessed March 28, 2023) (Bensch et al., 2009).

Despite their importance as pathogens potentially compromising avian host fitness and health (Atkinson et al., 1988; Merino et al., 2000; Garvin et al., 2003; Marzal et al., 2005; Palinauskas et al., 2008, 2009; Knowles et al., 2010; Puente et al., 2010; Lachish et al., 2011; Asghar et al., 2015), remarkably little is known about the parasites' exo-erythrocytic development. Before the parasites infect blood cells and develop gametocytes, they replicate asexually in the tissues of their hosts. During merogony, the parasites form exo-erythrocytic or tissue stages - so called meronts and, in the cases of Haemoproteus and Leucocytozoon, megalomeronts, which, depending on the parasite and host species, can damage organs dramatically, leading to organ failure and death (Valkiūnas, 2005). While exo-erythrocytic development occurs in all haemosporidians, species of the three genera differ substantially in certain aspects of merogony but the detailed pattern of exo-erythrocytic development remains non-existent or fragmentary for most described species (Valkiūnas and Iezhova, 2017; Hernández-Lara et al., 2021). With respect to species number, this is particularly true for parasites of the genus Haemoproteus. Despite being prevalent in many well-sampled passerine birds (Peirce, 1981; Fallon and Ricklefs, 2008; Dimitrov et al., 2010; Mata et al., 2015; Ellis et al., 2020), tissue stages have only been characterized for a fraction of the 177 Haemoproteus spp. described so far (Valkiūnas and Iezhova, 2017). Data from previous studies indicate that Haemoproteus parasites develop different types of tissue stages - meronts, which usually do not exceed 50 µm in diameter and are covered by a thin wall, and megalomeronts, which were reported to reach up to 800 µm in size and usually display a thick capsular-like wall (Valkiūnas, 2005; Valkiūnas and Jezhova, 2017: Duc et al., 2021). Meronts and megalomeronts can be observed in different organs of their hosts, with many Haemoproteus spp. developing in multiple different tissues and others showing a preference for certain organs. For example, Haemoproteus minutus and Haemoproteus lophortyx often develop in skeletal and heart muscles, or in the gizzard muscles (Cardona et al., 2002; Valkiūnas and Iezhova, 2017; Ortiz-Catedral et al., 2019), while Haemoproteus attenuatus forms meronts exclusively in the lungs (Hernández-Lara et al., 2021). Moreover, variations in the location of tissue stages were found between lineages of the same species, e.g., the Haemoproteus majoris lineages hPHSIB1 and hPHYBOR04 develop megalomeronts mainly in kidneys, whereas megalomeronts of the H. majoris lineage hPARUS1 were also found in other organs (Ilgūnas et al., 2019b; Duc et al., 2020). However, due to limited data on exo-erythrocytic development being available from only a few species and lineages, the mechanisms mediating the appearance of different tissue stages or differences in the site of development remain poorly understood. For example, it is currently unknown whether variations observed in the merogonic pattern reflect parasite traits represented by phylogenetic distances among species or indicate phenotypic plasticity of species depending on host-parasite associations. This is deplorable because knowledge about the exo-erythrocytic patterns in avian hosts is crucial for understanding of the pathogenesis and development of haemosporidioses. Notably, megalomeronts of Haemoproteus parasites have been associated with fatalities not only in nonadapted but also in natural hosts (Baker et al., 2018; Groff et al., 2019; Ortiz-Catedral et al., 2019), illustrating that these parasites might be less benign to their hosts than previously assumed (Atkinson et al., 1991; Bennett et al., 1993, 1994). Further data on the exo-erythrocytic development of other species is needed to explore if it is feasible to make predictions about the exo-erythrocytic development in closely related parasites and host species.

The reasons for the paucity of data on exo-erythrocytic development of haemosporidians are related to the difficulties of designing experimental studies with these parasites and accessing their exoerythrocytic stages in living birds. Besides the detection of tissue stages in histological sections, which requires laborious processing of organ samples from dead birds, their correct identification and taxonomic assignment is challenging, especially in samples from wild birds, where co-infections predominate (Valkiūnas, 2005). Natural infections with two or more parasites from the same or different haemosporidian genera are common and can be as high as 86% in certain host species (Valkiūnas et al., 2003; van Rooven et al., 2013; Bernotienė et al., 2016; Marinov et al., 2017). In such cases, molecular screening using PCR-based methods might not reveal all lineages present in a sample (Jarvi et al., 2002; Pérez-Tris and Bensch, 2005; Valkiūnas et al., 2006), making it nearly impossible to link detected tissue stages correctly with molecular data. To overcome these diagnostic difficulties, different approaches have been used in the past to identify tissue stages in histological sections, including the use of morphological keys (Valkiūnas, 2005; Valkiūnas and Iezhova, 2017) and in situ hybridization (ISH) techniques applying genus-specific molecular probes (Dinhopl et al., 2011; Himmel et al., 2019, 2020, 2021; Ilgūnas et al., 2022). Moreover, laser capture microdissection (LCM) has been successfully applied to identify megalomeronts of the parasites (Ilgunas et al., 2019b). However, all these techniques were mostly applied to the genus level of identification, requiring further development to study samples with mixed intrageneric infections and advance our understanding of the exoerythrocytic part of the parasites' life cycles.

Extending previous methodologies, this study investigated coinfecting haemosporidian parasites and their exo-erythrocytic stages in naturally infected common chaffinches Fringilla coelebs. Common chaffinches are passerine birds of the family Fringillidae residing in the Western Palearctic with breeding grounds from North-Western Africa across Europe to Siberia (BirdLife International, https://www.birdlife.org, accessed April 5, 2023). This species has been extensively sampled in previous studies, demonstrating high haemosporidian prevalence in many regions (Valkiūnas, 2005; Mata et al., 2015; Santiago-Alarcon et al., 2016; Ellis et al., 2020). However, despite being host to diverse haemosporidian lineages, very few exo-erythrocytic stages have been reported in this bird species yet, with only one record of a single Haemoproteus sp. megalomeront found in an individual from Austria (Himmel et al., 2020) and a few records of Haemoproteus majoris megalomeronts found in five individuals from Lithuania (Duc et al., 2023a). This study used co-infecting Haemoproteus parasites of F. coelebs as model organisms, aiming to gain new information on the exo-erythrocytic development of haemosporidians by applying parasite species- and lineage-specific identification techniques.

2. Material and methods

2.1. Sample collection

Common chaffinches *F. coelebs* were collected at the Ventė Cape Ornithological Station (55°20'38.93"N, 21°11'34.05"E, https://www.vros.lt), Lithuania, in May 2019 and 2021, and in September 2020 using mist nets and a large 'Rybachy'-type funnel trap. From each bird, a blood sample was obtained by puncturing the brachial

vein with a sterile needle and collected using a heparinized microcapillary. Drops of blood were used for preparation of blood films immediately after withdrawal, and the remaining blood was used to prepare blood spots on filter papers (samples collected in 2019) or collected in SET buffer (samples collected in 2020) and stored at $-20~^{\circ}\text{C}$ for molecular analyses. After air-drying of blood films, they were fixed by quickly dipping the slides in absolute methanol, stained with 10% Giemsa solution, and screened microscopically for the presence of haemosporidian parasites following a standard protocol for the detection of avian haemosporidian parasites (Valkiūnas, 2005). Birds determined positive for haemosporidians by blood film microscopy were euthanized by decapitation and their organs collected for histological investigations; in the case of birds collected in 2021, tissue samples were also collected in 96% ethanol for molecular analyses.

2.2. Microscopic examination and parasite morphology

For morphological determination of parasite species, blood films were screened using an Olympus BX61 (Olympus, Tokyo, Japan) light microscope equipped with an Olympus DP70 digital camera, and images of parasite blood stages acquired using Analy-SIS FIVE software (Olympus). Morphological evaluation of observed parasite blood stages and parasite species identification were done using standard protocols and parasite characters according to Valkiūnas (2005).

2.3. Histological examination

Samples of the brain, lungs, liver, spleen, kidneys, proventriculus, gizzard, intestines, skeletal muscle, and heart were fixed in 10% neutral buffered formalin for 24 h (samples collected in 2020 and 2021) and up to 4 weeks (samples collected in 2019), dehydrated in an increasing series of 70-100% ethanol, clarified in xylene, and embedded in paraffin wax. Histological sections of 2-3 μm were cut from formalin-fixed paraffin wax-embedded (FFPE) tissue samples, stained with H&E, cover-slipped, and screened for exoerythrocytic stages at magnifications of 100x and 200x using an Olympus B51 light microscope equipped with an Olympus UC90 digital camera (Olympus, Tokyo, Japan). Detailed examination of exo-erythrocytic stages and acquisition of photographs were performed using higher magnifications (400x, 1000x) and the image software cellSens Entry (Olympus). Acquired photographs were adjusted for brightness and contrast, and assembled in Adobe Photoshop CC 2023 (Adobe, San José, CA, USA). Based on the photographs, exo-erythrocytic stages were measured using the ImageJ-based image processing package Fiji (Image J 1.53c, National Institutes of Health, Bethesda, MD, USA, downloaded at https://imagej.net/software/fiji, accessed February 20, 2023) (Schindelin et al., 2012). Exo-erythrocytic meronts were measured by their largest diameter. Unless otherwise stated, measurements are presented as mean ± S.D., followed by the number of measurements in parentheses.

2.4. Chromogenic ISH

In parallel to H&E staining of tissue sections, chromogenic ISH was performed to detect and identify exo-erythrocytic stages of haemosporidians. For genus-specific identification, ISH was applied following previously established protocols and genus-specific probes targeting the 18S rRNA of *Haemoproteus* spp. (Haemo18S), *Leucocytozoon* spp. (Leuco18S), and *Plasmodium* spp. (Plasmo18S) (Dinhopl et al., 2011; Himmel et al., 2019, 2021). From each bird, at least three sections with all tissues were separately incubated with the three probes to detect mixed intergeneric infec-

tions. To further identify exo-erythrocytic stages found in birds with mixed intrageneric Haemoproteus infections, species- and lineage-specific probes were designed based on 18S ribosomal DNA sequences of diverse haemosporidian parasites and lineages analysed in a previous study (Harl et al., 2019), complemented by 18S ribosomal sequences of additional lineages (Harl et al., 2023). To identify H. majoris parasites, the probe Hmaj18S (5'-GGC AAA ACT AGC CTT AGG CGA CG-3') was designed to target different lineages of the H. majoris group, including hPARUS1, hPHSIB1, hCCF5, hCWT4, hWW2, and hEMSPO03. In addition to the genus- and species-specific probes, lineage-specific probes were designed for the detection of Haemoproteus sp. lineage hROFI1 (ROFI1-18S, 5'-TTC CGC GAC AGC CAT AAC AAC CAC C-3'), Haemoproteus fringillae lineage hCCF3 (CCF3-18S, 5'-CAC ACT CCA CTA ATC GAG TTT ATA CCT TCC GA-3'), and Haemoproteus magnus lineage hCCF6 (CCF6-18S, 5'-ACG GCA AAG AAA CTT CGC TAT TTC AAG TC-3'). Specificity of the probes was checked in silico by selecting target regions with low chances of cross-hybridization with parasites other than the target lineage or species. To confirm the specificity of the probes and rule out cross-reactivity, all probes were tested by ISH, applying them separately on tissue samples containing the respective lineages in single and mixed infections, and on tissue samples containing parasites of other lineages, species, or genera as determined positive in the present and previous studies (Supplementary Table S1). The probes were commercially synthesized by Microsynth Austria (Microsynth, Vienna, Austria) including digoxigenin labels at the 3' ends. Sequences of all probes applied in this study are provided in Table 1.

ISH was performed according to a previously published protocol (Dinhopl et al., 2011). In brief, FFPE tissue sections were deparaffinized, rehydrated, and subjected to proteolysis with proteinase K (#03115828001, Merck KgA, Darmstadt, Germany), 3 μ g/ml, in tris-buffered saline at 37 °C for 40 min. Thereafter, sections were rinsed in distilled water, dehydrated in 96% and 100% ethanol, and air-dried before incubation with hybridization solution containing 1 ng/100 μ l of genus-specific or 10 ng/100 μ l of species-or lineage-specific digoxigenin-labelled probes. Hybridization was performed in a humid chamber overnight at 40 °C. After hybridization, sections were subjected to stringency washes in saline-sodium citrate (SSC) buffer (pH 7.0) and incubated with normal goat serum blocking reagent (VESCS-1000, Szabo-Scandic,

Table 1Oligonucleotide probes used for the detection of haemosporidian parasites by chromogenic in situ hybridization.

Probe	Sequence (5' to 3')	Target parasites and lineages	Reference
Haemo18S	GCT AAC CGT AGT	Haemoproteus	Himmel
	TAT AGT CGC CAT	(Parahaemoproteus) spp.	et al.,
	CTC		2019
Leuco18S	TAG GAC TCC CCA	Leucocytozoon (Leucocytozoon)	Himmel
	CTT GTC TTT TTC	spp.	et al.,
	TTG A		2019
Plasmo18S	CTT AAA CTT CCT	Plasmodium spp.	Himmel
	TGT GTT AGA CAC		et al.,
	ACA AT		2021
Hmaj18S	GGC AAA ACT AGC	Haemoproteus majoris	present
	CTT AGG CGA CG	(PARUS1, PHSIB1, PHYBOR04,	study
		CWT4, CCF5, EMSPO03)	
CCF3-18S	CAC ACT CCA CTA	Haemoproteus fringillae (CCF3)	present
	ATC GAG TTT ATA		study
	CCT TCC GA		
CCF6-18S	ACG GCA AAG AAA	Haemoproteus magnus (CCF6)	present
	CTT CGC TAT TTC		study
	AAG TC		
ROFI1-18S	TTC CGC GAC AGC	Haemoproteus sp. (ROFI1)	present
	CAT AAC AAC CAC C		study

Vienna, Austria) containing 10% Triton X-100 (#648466, VWR International, Vienna, Austria) for 30 min before application of anti-digoxigenin-AP Fab fragments (#11093274910, Merck KgA) at a concentration of 1:200 to detect the digoxigenin-labelled hybrids. Chromogenic detection of the parasite-probe hybrids was done using the colour substrates 5-bromo-4-chloro- 3indolyl phosphate (BCIP) (#11383221001, Merck KgA) and 4nitro blue tetrazolium chloride (NBT) (#11383213001, Merck KgA). After stopping the chromogenic reaction with tris-EDTA buffer (#1.08382 and #1.12029, Merck KgA), sections were counterstained with haematoxylin (#105174, Merck KgA) and mounted using Aquatex (#1.08562, Merck KGaA) and coverslips. For every ISH procedure, appropriate positive controls (Plasmodium sp., Haemoproteus sp., or Leucocytozoon sp. positive tissue samples for confirmation at genus level, and tissue sections positive for the target species or lineages as confirmed previously) were included.

2.5. Immunohistochemistry

For immunohistochemical staining of vascular endothelial cells, a rabbit polyclonal von Willebrand Factor (vWF) antibody (F3520, Sigma Aldrich, St. Louis, Missouri, USA) was used. Von Willebrand factor is a key marker for both mammalian and avian endothelial cells (Yablonka-Reuveni, 1989). The commercial antibody used (F3520) detects human vWF expressed in endothelia, megakaryocytes, and platelets, and was confirmed to cross-react with avian endothelial cells of some avian species previously (unpublished data). For immunohistochemical staining of smooth muscle cells present in the middle layer of blood vessel walls, a mouse monoclonal smooth muscle actin (SMA) antibody clone 1A4 (M0851, Dako, Agilent Technologies, Vienna, Austria), was used. This antibody detects the α -smooth muscle actin isoform expressed in vascular smooth muscle cells and capillary pericytes in vertebrates (Skalli et al., 1989; Alarcon-Martinez et al., 2018). Immunohistochemistry was performed with a LabVision Autostainer 360 (Fisher Scientific, Vienna, Austria). First, 2 µm tissue sections were deparaffinized and rehydrated. For antigen retrieval, sections were treated with 0.1% pronase E solution (P5147, Merck KGaA) for 20 min at 37 °C (vWF antibody) or 3 μg/ml of proteinase K (#03115828001, Merck KgA) in tris-buffered saline at 37 °C for 40 min (SMA antibody). To reduce unspecific background staining, endogenous peroxidase activity was blocked with 3% hydrogen peroxide (7722-84-1, H₂O₂ 30% ACM, Herba Chemosan, Vienna, Austria, diluted 1:10 in distilled water) for 5 min. A protein block (TA-125-PBQ, Ultravision Protein Block, Fisher Scientific) was applied for 10 min to prevent unspecific binding of the primary antibodies. Next, sections were separately incubated for 30 min with the different primary antibodies diluted to concentrations of 1:500 (vWF) and 1:1500 (SMA) using a ready-to use antibody diluent (#003218, Fisher Scientific). Thereafter, sections were incubated with horseradish peroxidase (HRP)-labelled polymer conjugated secondary antibodies (BrightVision Poly-HRP-antimouse (DPVM110HRP) or anti-rabbit (DPVR110HRP) IgGs, ImmonoLogic, Duiven, Netherlands). After every step, slides were rinsed with tris-buffered saline pH 7.6 with 20X Tween 20 (TBS TA-999-TT, Fisher Scientific). Chromogenic detection was done for 5 min using 3,3'-diaminodbenzidine (DAB) (TA-125-QHDX DAB Quanto, Fisher Scientific). Finally, sections were counterstained with Mayer's haematoxylin (TA-060-MH, Lab Vision, Fisher Scientific) 1:30 for 1 min, dehydrated, and mounted using Neo-Mount (#1.09016.0500, Merck KgA).

2.6. Combined ISH and IHC

For simultaneous visualization of parasite exo-erythrocytic stages and their intravascular location, double labelling was performed by combining ISH and IHC in one assay. First, parasite stages were labelled by ISH. Subsequently, IHC was carried out for immunostaining of blood vessel walls using the SMA antibody. ISH and IHC were performed as described above with the following three modifications to allow for integration of both techniques into one workflow. First, after proteolysis during the ISH, the dehydration step was skipped to preserve immunohistochemical antigenicity. Instead, sections were washed in distilled water for 5 min to stop proteolysis. Second, after stopping the chromogenic reaction at the end of the ISH procedure, sections were placed into PBS (pH 7.4) (P-4417, Merck KgA) for 10 min and then transferred to the IHC autostainer. Third, immunostaining was done starting with the peroxidase blocking step and following the rest of the IHC protocol.

2.7. LCM

To identify exo-erythrocytic stages not attributable to one of the detected lineages by ISH, LCM was performed. For LCM, FFPE sections were cut at 4 µm, mounted on 1.0 polyethylene naphthalate (PEN) nuclease-free MembraneSlides (Carl Zeiss, Oberkochen, Germany) and dried overnight in an oven at 50 °C. Next, sections were deparaffinized in xylene for 5 min twice and rehydrated each 1 min in 100%, 96% and 70% ethanol. For visualization of parasite stages, sections were stained with 1% cresyl violet acetate solution, dehydrated by dipping into 70% and 100% ethanol, and air-dried. For LCM of small meronts < 20 µm, tissue sections were first subjected to ISH to label the parasites and facilitate visualization during the LCM procedure. LCM was performed using a Zeiss PALM MicroBeam LCM system and the PALM RoboSoftware version 4.6. The parasite stages were identified microscopically with 40x or 63x objectives and dissected with the RoboLPC laser function by manually drawing a line around the region of interest (Fig. 1). Laser focus, cut energy and laser pressure catapulting (LCP) values were manually adjusted with cut energy and LCP ranging from 30-55. Dissected structures were catapulted by a laser pulse into 0.6 ml AdhesiveCap microcentrifuge tubes (Carl Zeiss). To obtain a sufficient amount of parasite tissue for subsequent DNA isolation, parasite stages of interest displaying the same morphology were pooled from multiple locations within the same organ but collected separately for each bird individual. Specifically, meronts were dissected from the brains of five birds; these pools contained tissue from a total area of approximately 5100-24,000 μm². Exo-erythrocytic stages found in blood vessels of the liver and lung of two birds were separately pooled; these pools contained tissues from a total area of approximately 3700–10,100 μm². Collected tissues were stored in the microcentrifuge tubes at 4 °C until DNA extraction.

2.8. DNA isolation

Total DNA was extracted from blood spots, blood in buffer, and frozen tissue using the DNeasy Blood & Tissue Kit (Qiagen, Venlo, Netherlands) following the manufacturer's instructions with one modification: the DNA was eluted twice with each 100 μ l of AE buffer, and the second eluate was used as PCR template.

For DNA extraction from formalin-fixed tissue obtained by LCM, the QIAamp DNA Micro Kit (Quiagen) was used following the manufacturer's protocol for isolation of genomic DNA from laser-microdissected tissues. Proteinase K digestion was performed overnight to ensure good proteolysis.

2.9. PCR

2.9.1. Blood and tissue samples

Samples were screened for haemosporidian parasites using a nested PCR protocol targeting a 478 bp fragment of the mitochondrial *cytb* gene (Hellgren et al., 2004). The outer primer pair

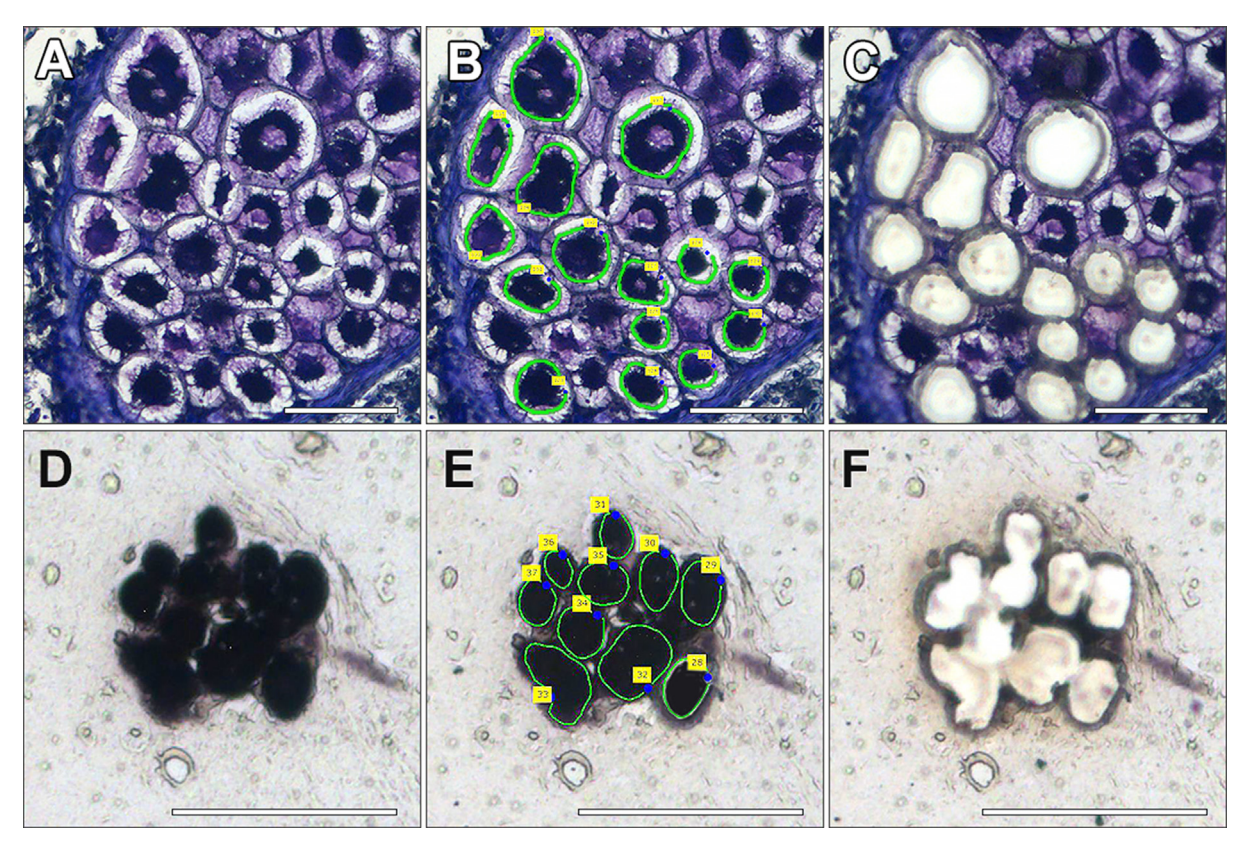


Fig. 1. Laser microdissection of *Haemoproteus* spp. meronts from lung (A-C) and brain (D-F) sections of *Fringilla coelebs*. (A) A cluster of meronts in a pulmonary vessel prior to laser dissection. (B) Marking of cutting lines around the meronts for guiding the laser beam. Note that only meronts with intact covering membranes were selected to avoid contamination with blood cells. (C) The same meront cluster after ablation of the selected meronts. (D) A group of meronts in a brain section, labelled by the *Haemoproteus* genus-specific in situ hybridization (ISH) probe. (E) Cutting lines around each meront for laser beam guidance. (F) The same brain section after ablation of the selected meronts. Scale bars = 50 μm.

HaemNFI/HaemNR3 was used to amplify DNA of Plasmodium, Haemoproteus, and Leucocytozoon. In the nested PCR using 1 µl of amplicon from the first PCR product, the inner primer pairs HaemF/HaemR2 and HaemFL/HaemR2L were used to amplify DNA of Plasmodium/Haemoproteus, and Leucocytozoon, respectively. PCRs were performed in 25 µl reaction volumes containing 14.375 µl of nuclease-free water, 5 µl of 5X Green GoTaq Flexi Buffer (Promega, Madison, Wisconsin, USA), 2 µl of MgCl₂ solution (25 mM), 0.5 µl of PCR nucleotide mix (10 mM, Promega), 0.125 µl of GoTaq G2 Flexi DNA Polymerase (5 u/µl, Promega), 1 μl each of forward and reverse primers (10 pmol/μl), and 1 μl of DNA template. PCRs were run as follows: an initial step of 2 min at 94 °C, followed by 35 cycles of 30 s at 94 °C, 30 s at 50 °C, and 1 min at 72 °C, followed by a 10 min final extension at 72 °C. PCR amplifications were checked by gel electrophoresis of nested PCR products run on 1% agarose gels stained with Midori Green Advance (Nippon Genetics Europe, Dueren, Germany) and visualization of amplicons using a BioSens SC-Series 710 gel documentation system (GenXpress, Wiener Neudorf, Austria). In every PCR run, a haemosporidian-positive and a negative (nuclease-free water) control were included. PCR-positive samples were sent for bi-directional sequencing to Microsynth Austria.

2.9.2. Laser microdissected tissue samples

To overcome difficulties with amplification of longer DNA fragments from formalin-fixed, laser microdissected tissue samples, three primer pairs were designed which amplify overlapping fragments of the *cytb* gene, resulting in a 566 bp fragment which includes the full 478 bp barcode region (Fig. 2). The first pair comprised the primers CytbSF1 (5-GAG AAT TAT GGA GTG GAT GGT-3)

and CytbSR1 (5-CAC CCC AGA AAC TCA TTT G-3), the second pair the primers CytbSF2 (5-ATG GGT TAT GTA TTA CCT TGG G-3) and CytbSR2 (5-GGA TAG AAA GGT ATT TTT AAA GCT GTA-3), and the third pair the primers CytbSF3 (5-AGC ACT AAT CCT TTA GGG TAT G-3) and CytbSR3 (5-GCA TAG AAA GGT AAG AAA TAC CA-3).

LCM tissue samples were screened with all three primer pairs. PCRs were performed in 25 µl reaction volumes containing 7.5 µl of nuclease-free water, 12.5 µl of Kapa2G Fast HotStart ReadyMix (Kapa Biosystems, Wilmington, Massachusetts, USA), 1 µl of MgCl₂ solution (25 mM), 1 µl each of forward and reverse primers (10 pmol/µl), and 2 µl of DNA template. The following thermoprofile was used: an initial step of 3 min at 95 °C, followed by 40 cycles of 15 s at 95 °C, 15 s at 50 °C, and 30 s at 72 °C, followed by a 5 min final extension at 72 °C. Positive and negative controls were included in every PCR run. The success of PCR amplification was checked by gel electrophoresis of 5 µl of PCR products loaded on 1% agarose gels stained with Midori Green Advance (Nippon Genetics Europe). PCR-positive samples were sent for bidirectional sequencing to Microsynth Austria. In cases of samples showing no amplification, the remaining PCR products (20 µl per sample) were again loaded on 1% agarose gels, rerun, and exised for gel extraction, and the extracts used as templates for a second round of amplification. For the gel extraction, slices of gels (approximately 300 μg of gel for each sample) were excised with a sterile spatula from the sample lanes at the expected DNA fragment size, using the band of the positive control as a reference for the fragment length. Excised DNA fragments were transferred into microcentrifuge tubes and purified with the QIAquick gel extraction kit (Quiagen) according to the manufacturer's protocol. DNA was eluted with 30 µl of elution buffer. For re-amplification,

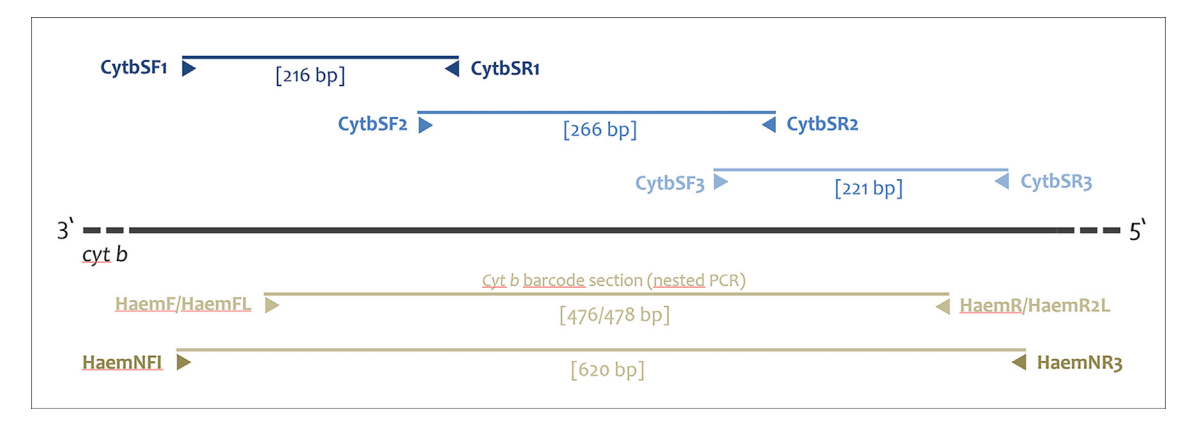


Fig. 2. Schematic illustration of the location and directions of primers designed to amplify partial cytochrome b (*cytb*) gene of avian haemosporidians of the genera Plasmodium, Haemoproteus, and Leucocytozoon. Three primer pairs (CytbSF1/ CytbSR2, CytbSF2/CytbSR2, and CytbSF3/CytbSR3) were designed to amplify short overlapping fragments of the *cytb* gene, covering the 478 bp long barcode section amplified by primers of the nested PCR protocol according to Hellgren et al. (2004).

2 µl of purified DNA were subjected to a second PCR using the same primers and conditions as in the first PCR. DNA amplification was checked by gel electrophoresis and positive samples were sent for bi-directional sequencing to Microsynth Austria (Microsynth).

2.10. Sequence analysis

Sequences and electropherograms were analysed with the sequence alignment software Bioedit v.7.0.5.3 (downloaded at https://bioedit.software.informer.com/, accessed August 24, 2022) (Hall, 1999). Sequences containing ambiguous characters, indicating co-infections, were carefully checked and unphased using DnaSP v.6.12.3 (downloaded at https://www.ub.edu/dnasp/, accessed August 24, 2022) (Rozas et al., 2017). All sequences were subjected to BLAST searches in the avian malaria database MalAvi (Lund University, Lund, Sweden, https://130.235.244.92/Malavi/, accessed February 6, 2023) (Bensch et al., 2009) and NCBI GenBank. Nucleotide sequences of detected haemosporidians were uploaded to GenBank under the accession numbers OR250625-OR250656.

2.11. Phylogenetic analysis

A phylogenetic tree of *Haemoproteus* spp. of the subgenus *Parahaemoproteus* was calculated with lineages detected in this study and lineages from all *Parahaemoproteus* spp. for which a 478 bp *cytb* barcode was available. In the case of morphospecies with several linked lineages, only the most common lineage was selected for calculation of the tree. In total, the alignment contained 68 *Haemoproteus* lineages, including lineages of 60 *Parahaemoproteus* spp. and seven lineages detected in this study. A sequence of *Haemoproteus columbae* hHAECOL1 of the subgenus *Haemoproteus* was used as the outgroup.

A Maximum Likelihood (ML) bootstrap majority rule consensus tree (10,000 replicates) was calculated with IQ-TREE v.1.6.12 (Trifinopoulos et al., 2016), applying the best-fit model GTR + G + I. A Bayesian Inference (BI) tree was calculated with MrBayes v.3.2.2 (Ronquist et al., 2012). The BI analysis was run for 5 million generations (two runs with four chains, one of which was heated), sampling every thousandth tree. The first 25% of the trees were discarded as burn-in and a majority rule consensus tree was calculated from the remaining 3,750 trees. The tree was visualized with Figtree v.1.4.4 (https://tree.bio.ed.ac.uk/software/figtree/; Andrew Rambaut) and edited with Adobe Illustrator CC v.2015 (Adobe Inc.).

3. Results

3.1. Fringilla coelebs show high rates of co-infections dominated by Haemoproteus spp.

Molecular screening revealed haemosporidian lineages from all three genera, although Haemoproteus parasites were most prevalent with 19 of 20 birds infected. Five birds showed infections with Leucocytozoon, and one bird was infected with Plasmodium (Table 2). Combining the results from standard nested PCR screening (Hellgren protocol), LCM, and ISH, 15 of 20 (75%) birds showed co-infections, including nine double infections and five triple infections. One bird (AH2168) was infected with five lineages, considering the sequencing results obtained by cloning the parasites' 18S rRNA gene from a sample of this bird analysed in a previous investigation (Harl et al., 2023). In total, nine cytb lineages were found, including seven lineages of the genus Haemoproteus, and one lineage each of the genera Plasmodium and Leucocytozoon. Among Haemoproteus parasites, Haemoproteus magnus hCCF6 (molecularly characterized in section 3.2), was most prevalent with 10 (50%) infected birds, followed by Haemoproteus fringillae hCCF3 in seven birds, Haemoproteus sp. hROFI1 in six birds, and Haemoproteus majoris hCCF5 in five birds. The Haemoproteus lineages hCCF2 and hCCF1 were found in four and two individuals, respectively, and H. magnus hCCF09 (molecular characterization in section 3.3) was found once. Among the five Leucocytozoon-infected birds, two showed infections with Leucocytozoon sp. lBRAM3, while in the remaining three birds the lineages were not identified, as they were positive for Leucocytozoon blood stages only by ISH. Plasmodium circumflexum pTURDUS1 was detected in one bird. All lineages were previously reported. Notably, in half of the birds, the nested PCR protocol failed to amplify lineages later identified by LCM, and/or ISH (Table 2). This particularly pertained to the lineage hROFI1, which was missed in five of six cases, and the lineage hCCF2, which was missed in two of four cases. Similarly, Leucocytozoon sp. was not detected by standard PCR screening in three of five cases, and *H. majoris* hCCF5 was missed in one of five birds.

3.2. Molecular characterization of H. magnus

Gametocytes present in the hCCF6 infections displayed the main *H. magnus* characteristics (Fig. 3A-E): the gametocytes grow around the erythrocytes' nuclei, markedly enclose them with ends (Fig. 3A, B, D) but only slightly (if at all) displace the nuclei laterally (Fig. 3A-E); the largest gametocytes tend to be close to circumnuclear in form (Fig. 3C, E); dumbbell-shaped growing gametocytes

Table 2Haemosporidian parasites, their cytochrome b (cytb) lineages and exo-erythrocytic stages detected in Fringilla coelebs by PCR screening, laser capture microdissection (LCM), and in situ hybridization (ISH).

Bird	Collection date	Parasite species and cytb lineages detected			Exo-erythrocytic stages detected and their attribution to species and lineages based on ISH probe reactivity and LCM results $^{\rm c}$						
		PCR ^a	ISH ^b	LCM b	Heart	Lung	Liver	Kidney	Brain	Gizzard	Muscle
AH1965	2019-05-04	Haemoproteus fringillae hCCF3, Haemoproteus magnus hCCF6, Leucocytozoon sp. IBRAM3			-	MM (hCCF6), meronts (hCCF3)	-	MM (hCCF6)	-	-	-
AH1968	2019-05-05	Haemoproteus sp. hCCF2, Leucocytozoon sp. IBRAM3	Haemoproteus sp. hROFI1		MM (H. sp.)	-	-	-	meronts (hROFI1)	-	-
AH1972	2019-05-07	H. fringillae hCCF3, H. magnus hCCF09			-	meronts (hCCF3)	-	-	-	-	-
AH1973	2019-05-07	Haemoproteus majoris hCCF5	Haemoproteus sp. hROFI1, H. fringillae hCCF3		-	meronts (hCCF3)	-	-	meronts (hROFI1)	-	-
AH1975	2019-05-11	H. fringillae hCCF3, H. majoris hCCF5	Haemoproteus sp. hROFI1		MM (hCCF5)	-	-	-	meronts (hROFI1)	-	-
AH2150	2020-09-18	H. majoris hCCF5			-	-	-	-	-	-	-
AH2151	2020-09-19	Haemoproteus sp. hCCF2			-	-	-	-	-	-	-
AH2152	2020-09-19	H. magnus hCCF6			_	_	_	_	_	_	_
AH2153	2020-09-20	H. magnus hCCF6	Leucocytozoon sp.		-	-	-	-	-	-	-
AH2154	2020-09-21	H. magnus hCCF6	Sp.		_	_	_	_	_	_	_
AH2155	2020-09-21	H. magnus hCCF6	Leucocytozoon sp.		-	-	-	-	-	-	-
AH2156	2020-09-28	Plasmodium circumflexum pTURDUS1	Leucocytozoon sp.		-	-	-	-	-	-	-
AH2167	2021-05-20	Haemoproteus sp. hCCF1		Haemoproteus sp. hCCF2	-	meront cluster (hCCF2)	-	-	-	-	meron cluster (hCCF2
AH2168	2021-05-20	H. majoris hCCF5, H. fringillae hCCF3 d H. magnus hCCF6 d	Haemoproteus sp. hROFI1	Haemoproteus sp. hCCF2, Haemoproteus sp. hROFI1	MM (hCCF5)	meront	meront cluster (hCCF2)	-	meronts (hROFI1)	-	_
AH2169	2021-05-20	H. magnus hCCF6, Haemoproteus sp. hROFI1		sp. likorii	-	- (IICCF3)	-	MM (hCCF6)	meronts (hROFI1)	-	-
AH2171	2021-05-20	Haemoproteus sp. hROFI1, H. magnus hCCF6 ^d	Haemoproteus sp. hROFI1	Haemoproteus sp. hROFI1	-	-	-	-	meronts (hROFI1)	-	-
AH2172	2021-05-20	H. majoris hCCF5, H. fringillae hCCF3			-	meronts (hCCF3)	-	-	-	-	-
AH2173	2021-05-20	H. fringillae hCCF3, H. magnus hCCF6			-	meronts (hCCF3)	-	-	-	-	-
AH2174	2021-05-20	H. fringillae hCCF3, H. magnus hCCF6	H. majoris		-	MM (hCCF6)	-	-	-	MM (H. majoris)	-
AH2176	2021-06-04	Haemoproteus sp. hCCF1			-	-	-	-	-	-	-

^a PCR using the nested PCR protocol by Hellgren et al. (2004).

were not seen; pigment granules were predominantly oval or elongate (Fig. 3B, D, E), of large (1–1.5 μ m) or medium (0.5–1 μ m) size, and randomly scattered. Identical morphological characters were seen in gametocytes of the closely related lineage hCCF09. Morphology of observed *H. magnus* gametocytes in both these lineages was the same as described before (Valkiūnas, 2005), and it is not repeated here. Voucher blood films with gametocytes of *H. magnus* (lineage CCF6, accession numbers 49,633 – 49,638 NS) and *H. magnus* (lineage CCF09, accession numbers 49639–49641 NS) were deposited in the Nature Research Centre, Vilnius.

3.3. Phylogeny

Phylogenetic reconstruction of *Haemoproteus* (*Parahaemoproteus*) spp. using 478 bp *cytb* sequences returned a basal polytomy with seven clades, three of which were moderately to strongly supported (BI posterior probability ≥ 0.85 / ML bootstrap support ≥ 95) (Fig. 4). Four of the *Haemoproteus* lineages detected in this study – hROFI1, hCCF1, hCCF2, and hCCF3 – clustered in a clade with moderate support (0.74/90), which comprised lineages of at least 14 morphospecies, including *Haemoproteus dumbbellus*, *Haemoproteus*

^b Given are only lineages which were additionally detected by LCM or ISH using genus- (*Haemoproteus*, *Leucocytozoon*), species- (*H. majoris*), and lineage- (hCCF3, hCCF6, and hROFI1) specific probes.

c Organs which remained negative for exo-erythrocytic stages in all birds were excluded from the table. MM, megalomeronts; -, no exoerythrocytic stages detected.

d Lineages were identified by cloning the parasites' 18S ribosomal DNA sequences during a previous study (Harl et al., 2023).

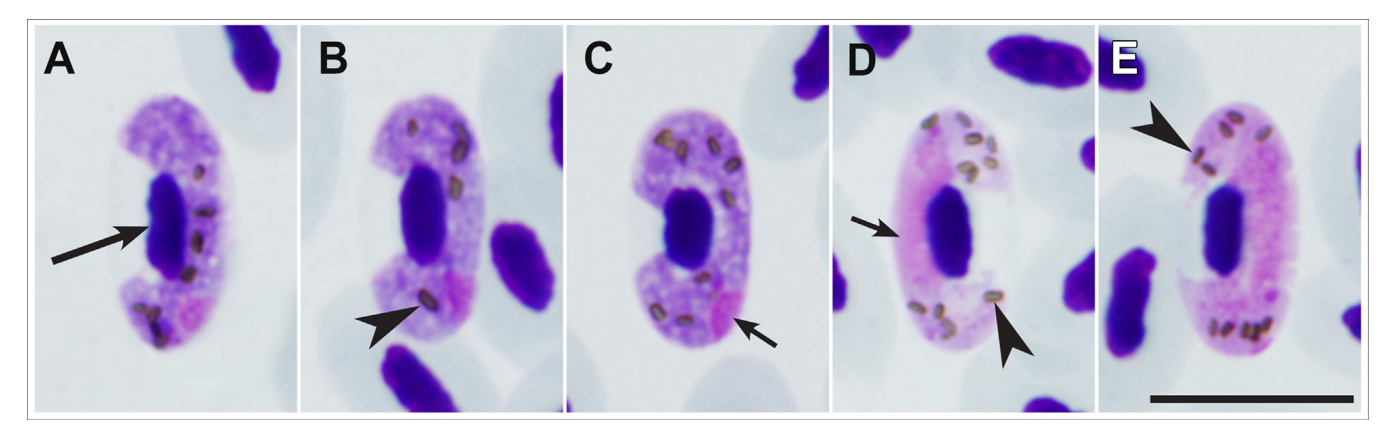


Fig. 3. Gametocytes of *Haemoproteus magnus* (lineage CCF6) from the blood of *Fringilla coelebs*. (A-C) Macrogametocytes, (D, E) microgametocytes. Note that elongate large pigment granules are present in (B) advanced gametocytes – an important and readily recognisable character of this parasite species. Long simple arrows indicate host cell nuclei, short simple arrows indicate parasite nuclei, and simple arrowheads indicate pigment granules. Methanol-fixed, Giemsa-stained blood films. Scale bar = 10 μm.

passeris, and Haemoproteus tartakovskyi. Within this clade, the lineages hCCF1 and hCCF2, differing by five bp or 1% in the cytb barcode region, grouped in a strongly supported clade (0.99/96), indicating close relationships. The lineage hCCF5 clustered with hPARUS1, a lineage of *H. majoris*, however, their evolutionary relationship to other Parahaemoproteus spp. was not resolved as the basal node only obtained low support values (0.58/58). The lineages hCCF09 and hCCF6 were nested in a separate clade with low support (0.51/62). They differ from each other by one bp (0.2%) in the cytb barcode, forming their own group (0.99/100) in the tree, and by one bp from *H. magnus* hCCF7, which was not included in the tree due to its shorter length of only 380 bp. According to the phylogenetic analysis, Haemoproteus lanii hRBS4 was the closest parasite to *H. magnus* hCCF09/hCCF6, differing by 17 bp (3.6%) in the cytb barcode.

3.4. Histological and ISH analysis using lineage-specific probes reveals different host tissue tropism of Haemoproteus parasites

Twelve birds showed *Haemoproteus* tissue stages in various organs, including the lungs, liver, kidneys, brain, heart and skeletal muscle, and gizzard (Table 2). The tissue stages were detected by ISH using the *Haemoproteus* genus-specific probe, and many of them were also found in corresponding H&E-stained sections. In six birds, multiple tissue stages were found, which varied in morphology and organ distribution. Most of these tissue stages were further identified to species or lineage level by ISH using species-specific and lineage-specific probes, or by LCM and subsequent PCR and sequencing. In the cases of the *Plasmodium*- and *Leucocytozoon*-infected birds only blood stages but no tissue stages of the respective parasites were seen.

3.5. Description of exo-erythrocytic stages

3.5.1. Haemoproteus sp. hROFI1 develops meronts exclusively in the brain

Six birds showed multiple meronts in sections of their brains (Fig. 5). The meronts were labelled by the *Haemoproteus* genusspecific probe during ISH. Because these birds were infected with different *Haemoproteus* lineages according to the PCR results, brain sections from five of them were subjected to LCM followed by PCR and sequencing to identify the parasite lineage forming the observed meronts. In three birds, PCR and sequencing of the microdissected meronts was successful, revealing the *Haemoproteus* lineage hROFI1. PCR of the microdissected meronts from the brain of the other two individuals was unsuccessful, but ISH using

the hROFI1 lineage-specific probe showed labelling of the meronts in all six individuals, confirming that all meronts found in the brains of the birds belonged to this lineage.

In all birds, the Haemoproteus sp. hROFI1 meronts showed a multifocal distribution across different regions of the brain, including cerebrum, midbrain, and cerebellum. The number of detected meronts varied among individuals, ranging from less than 10 to more than 100 meronts per brain section. Meronts located in different brain areas were commonly observed in close spatial association with one another (Fig. 5A), or in small groups with multiple meronts closely adjoining each other (Fig. 5G-L). The meronts were roundish, oval, or elongated. In longitudinal cuts of smaller vessels, meronts were often seen to infect neighbouring endothelial cells (Fig. 5B, C, D, E). Meronts closely adjoining in groups were usually round, although elongate cuts were also observed (Fig. 5J). The meronts located in endothelial cells, as demonstrated by positive IHC staining of vWF expressed in endothelial cells (Fig. 5C, I). The diameter of individual meronts ranged from 7-50 μ m (16.3 \pm 6.8 μ m, n = 58). Detected meronts varied in their stages of development. Young meronts stained basophilic with barely recognizable nuclei (Fig. 5E). Occasionally, small, roundish vacuoles were seen in growing meronts (Fig. 5E). In meronts more advanced in their development, merozoites were discernible (Fig. 5D), and cytomere formation was observed (Fig. 5F, J, K, L, O). Asynchronous development of adjacent meronts was seen (Fig. 5J, K, I, O). Mature meronts showed numerous discrete, round merozoites of approximately 1 μ m (1.1 \pm 0.1 μ m, n = 50) in size (Fig. 5K). The meronts were frequently accompanied by mild to moderate reactive gliosis and perivascular infiltration with mononuclear inflammatory cells (Fig. 5E, O). Occasionally, meronts were closely associated with multinucleated giant cells, which seemed to engulf the parasite stages (Fig. 5M, N).

3.5.2. Haemoproteus sp. hCCF2 develops meront clusters in the vascular system

In two birds (one infected with *Haemoproteus* spp. hCCF2 and hROFI1, and the other infected with *Haemoproteus* spp. hCCF1, hCCF2, and hROFI1), numerous merogonic stages were observed in the lumen of larger blood vessels (100–500 µm in diameter) of the lungs and the liver (Fig. 6 and Supplementary Fig. S1), and in one bird also in a vessel of the skeletal muscle (Supplementary Fig. S1). The merogonic stages appeared in multiple individual compartments, each containing a merogonic body which was covered by a thin membrane. These compartments were closely aggregated, forming compact clusters of multiple individual meronts inside the vascular lumen. They were stained by the *Haemoproteus*

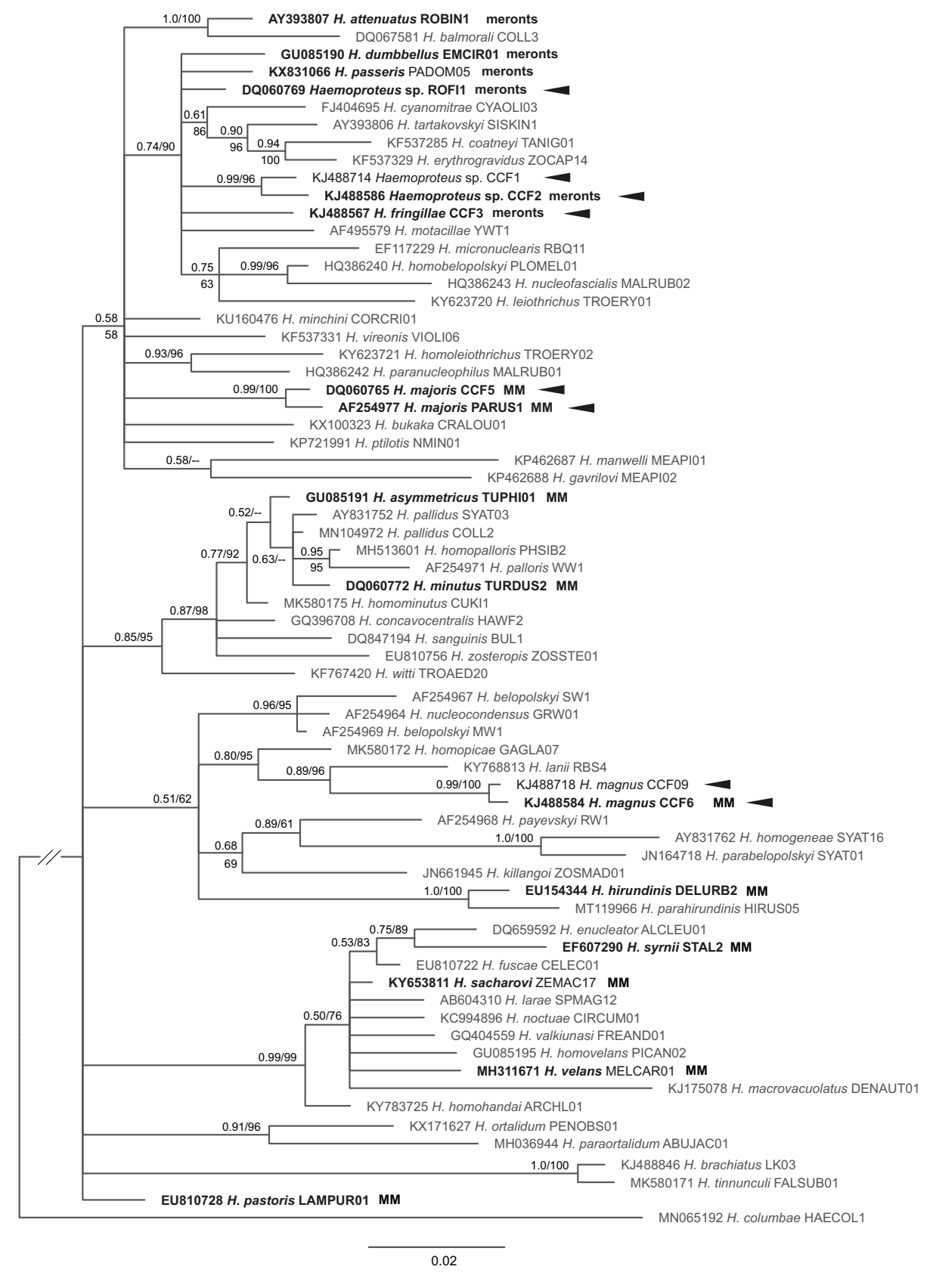


Fig. 4. Bayesian inference tree of 68 *Haemoproteus* cytochrome b (*cytb*) gene lineages (487 bp). Except for lineages detected in the present study (marked by arrows), only lineages which have been linked to morphospecies were included in the analysis. A sequence of *H. columbae* hHCOEL1 was used as outgroup. Parasites species and lineages, for which exo-erythrocytic stages have been reported in this and previous studies, are provided in bold, with the type of tissue stages found (meronts or megalomeronts (MM)). Bayesian inference posterior probabilities and Maximum-likelihood bootstrap values and are indicated at each node. The scale bars indicate the expected number of substitutions per site according to the model of sequence evolution applied. For all lineages, GenBank accession numbers were provided, followed by species and lineage names according to the Malavi database (http://130.235.244.92/Malavi/, accessed January 11, 2023).

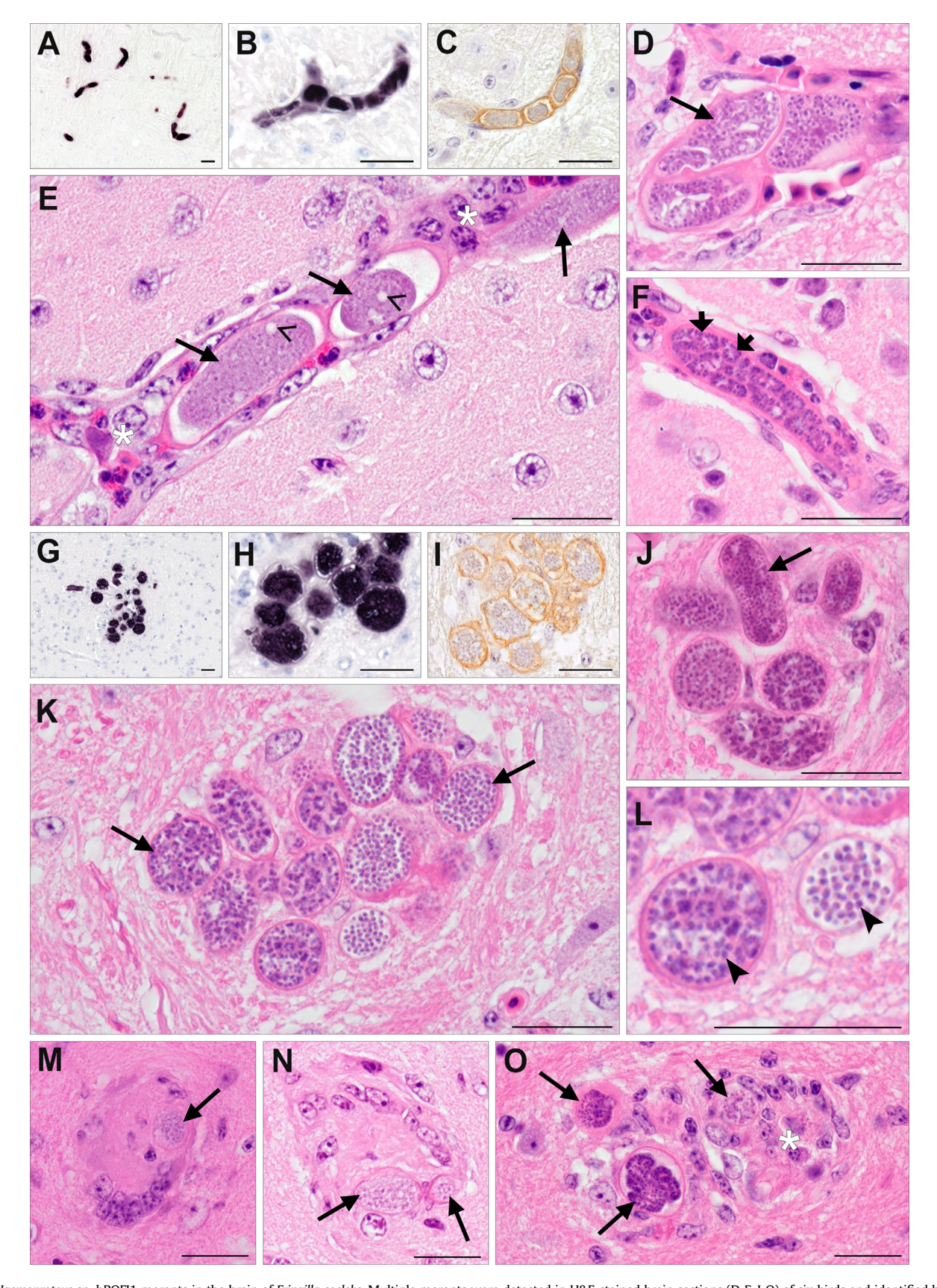


Fig. 5. Haemoproteus sp. hROF11 meronts in the brain of Fringilla coelebs. Multiple meronts were detected in H&E-stained brain sections (D-F, J-O) of six birds and identified by in situ hybridization (ISH) using a hROF11 lineage-specific probe (A-B, G-H). They were found in capillaries in close spatial association (A), or adjoining in small groups (G, J-L). Meronts located intracellularly in endothelial cells, demonstrated by immunohistochemical labelling—brown diaminobenzidine (DAB) of von Willebrand Factor, a marker for endothelial cells (C, I). Meronts often infected neighbouring endothelial cells (B-E). Meronts varied in their stage of maturity; young meronts lacked recognizable nuclei but displayed vacuoles (E), meronts more advanced in their development were characterized by cytomere formation (F), whereas nearly mature and mature meronts showed numerous merozoites (J-L). Moronts were associated with perivascular inflammation (E), reactive gliosis (O), and occasionally multinucleated giant cells, which seemed to engulf the parasite stages (M-N). → meront; →, cytomere; →, merozoite; →, vacuole; ⋆, perivascular inflammation (E) and gliosis (O). Scale bars = 20 μm.

genus-specific probe, and LCM of several meronts from these clusters revealed the lineage hCCF2 in all cases. Occasionally, intermingling blood cells were observed between neighbouring compartments containing merogonic stages more advanced in differentiation (Fig. 6G, K, L). No capsule-like wall was seen around the clustering meronts.

The entire meront clusters varied in size, with the biggest spanning 637 µm at its largest diameter. Cross-sections through some of the larger clusters revealed an almost concentric arrangement of two types of merogonic stages, which differed in size, morphology and by their reactivity with the ISH probe (Fig. 6A-D and Supplementary Fig. S1B-D, I, J). Merogonic stages observed in the inner core of the cluster were small and closely appressed with no or little space around them. These stages were roundish or oval, ranging from 12–24 μ m (14.8 \pm 2.4 μ m, n = 25) in size, and were characterized by a multinucleated mass of cytoplasm (Fig. 6C, D and Supplementary Fig. S1B-D. I. I). They stained bright eosinophilic (Fig. 6A. C, D) but were unreactive during ISH (Fig. 6B and Supplementary Fig. S1B-D, I, J). Merogonic stages at the periphery of the clusters were usually larger and advanced in differentiation, showing aggregations of numerous nuclei (Fig. 6C-D, K-L). Developing meronts showed cytomere formation (Fig. 6D). These meronts ranged from 14–46 μ m (27.8 \pm 6.9 μ m, n = 98) in size and were well delimited from one another by a thin covering membrane, assuming roundish or polygonal shapes. A large space separated the meronts from their covering membranes and often, small round vacuolic spaces were seen (Fig. 6K, L). At high magnification, fine, meshlike projections spanned the space between the meronts and their covering membranes (Fig. 6L). These meronts were strongly labelled by ISH (Fig. 6B, J and Supplementary Fig. S1B-D, F, I, J, L). Mature meronts contained well differentiated, discrete merozoites (Fig. 6H), which were 1.2 \pm 0.1 μ m (n = 30) in size. These only showed weak or no labelling by ISH (Fig. 6F). Among mature meronts, several ruptured compartments were observed with merozoites released and scattered (Fig. 6H).

The hCCF2 meront clusters were located in arteries and veins. Immunohistochemistry using an antibody against smooth muscle cell actin confirmed the intravascular location of the clusters (Fig. 6B, F, J and Supplementary Fig. S1F, I, J). In most cases, the meront clusters completely occupied the vascular lumen. Within the vessels, the clusters were surrounded by numerous leucocytes. In a pulmonary artery containing a cluster of multiple intact and ruptured merogonic compartments, the formation of a large intravascular thrombus was observed (Fig. 6E). Multiple intravascular multinucleated giant cells were observed alongside another meront cluster found in a pulmonary vein (Supplementary Fig. S2). Mild to moderate mixed inflammatory infiltrates were seen around affected vessels in the liver and the lungs (Fig. 6I and Supplementary Fig. S1A-C).

3.5.3. Haemoproteus magnus hCCF6 develops megalomeronts in kidneys and lungs

Three birds infected with *H. magnus* hCCF6 and other lineages showed multiple megalomeronts in the kidneys, and one of them also in the lung (Fig. 7). ISH using the *Haemoproteus*-specific probe confirmed the generic origin for most detected stages. Several megalomeronts found in additional sections prepared from these individuals were labelled by the hCCF6-specific probe, identifying them as *H. magnus* hCCF6.

The megalomeronts varied in size and maturation but all of them lacked a capsule-like wall typical for big *Haemoproteus* spp. megalomeronts. They were roundish to oval but irregular shapes were also observed.

In the kidney, early merogonic stages were located intracellularly in tubular epithelial cells (Fig. 7A-C). They were oval and $16.2 \pm 3.4 \, \mu m$ (n = 3) in size, and stained homogenously basophilic.

These small stages were labelled by the hCCF6-specific probe. Growing megalomeronts more advanced in their development showed formation of roundish to irregular-shaped cytomeres (Fig. 7D-W). They ranged from 29–76 μ m (46.7 \pm 13.4 μ m, n = 13) in their largest diameter. The cellular location of these megalomeronts could not be determined as the infected host cells and their nuclei were not discernible. A single mature (or nearly mature) megalomeront was observed in the kidney of one bird (Fig. 7S, T). It contained numerous discrete merozoites which were 1.1 \pm 0.1 μ m in size and arranged in barely recognizable cytomeres.

Megalomeronts found in the lungs ranged from 39–154 μ m (93. 1 ± 21.9 μ m, n = 4) at their largest diameter and showed different stages of maturity. Developing megalomeronts showed roundish cytomeres, but merozoites were not yet recognizable (Fig. 7U-W). Mature megalomeronts found in the lungs morphologically resembled those found in the kidney and were filled with numerous well defined merozoites (Fig. 7X, Z). Mature megalomeronts found in the kidney and lungs were unreactive to the ISH probes (Fig. 7Y).

A mild to moderate inflammatory reaction was observed around several megalomeronts (Fig. 7], M, Q, X).

3.5.4. Haemoproteus majoris develops megalomeronts in the heart, lungs, and gizzard

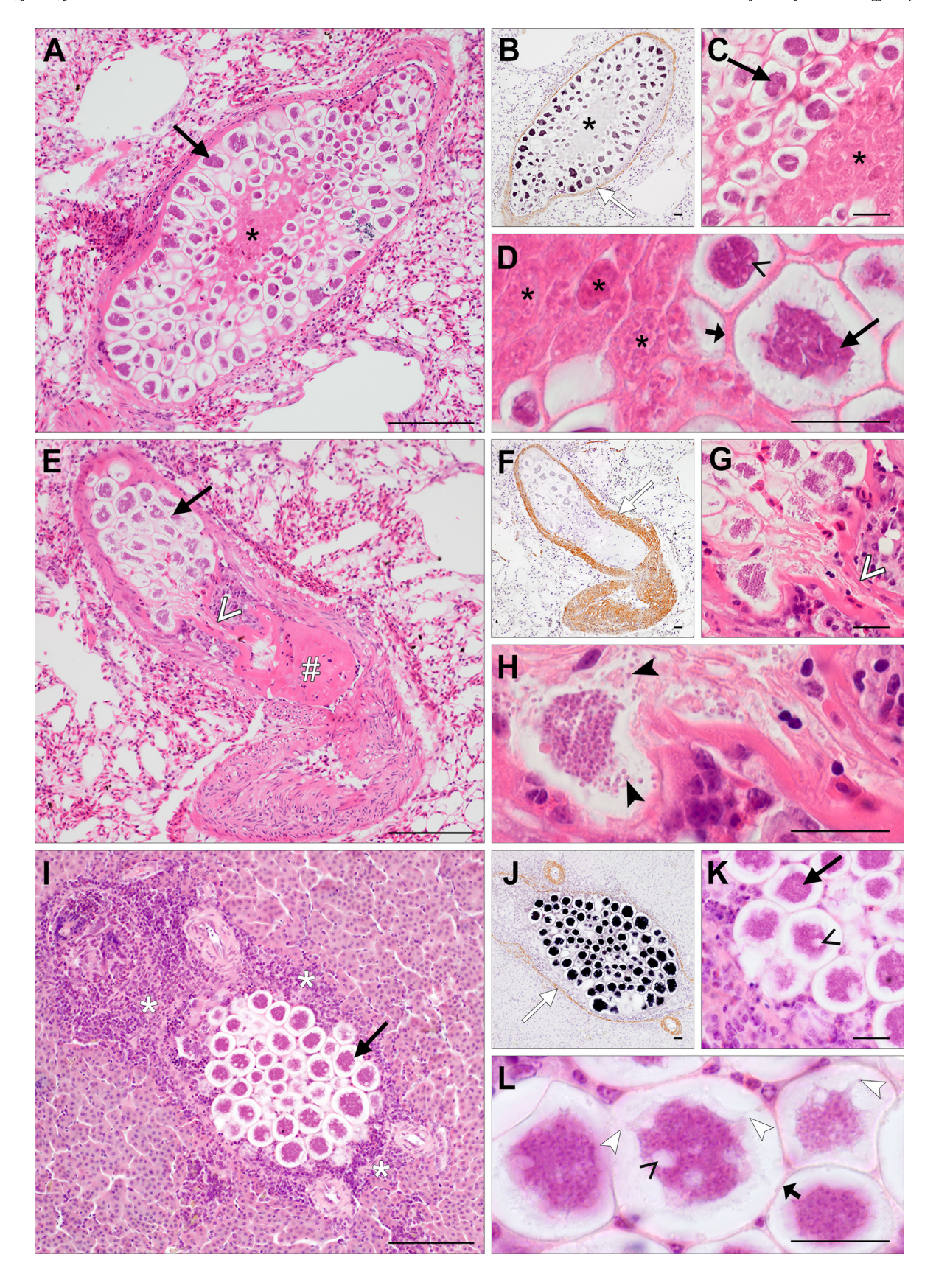
In three birds, growing megalomeronts of *H. majoris* were found (Fig. 8). Their species identity was confirmed by ISH using the *H. majoris* species-specific probe. In two birds, both infected with *H. majoris* hCCF5, a few megalomeronts were found in the heart muscles (Fig. 8A-H), and a single megalomeront was also observed in the lung of one of the two individuals (Fig. 8I-L). In the third individual, a single megalomeront was found in the muscular layer of the gizzard (Fig. 8M-P). In this bird, no *H. majoris* lineage was detected by PCR. Because no additional megalomeronts were found in subsequent tissue sections, the lineage of this megalomeront could not be determined.

Apart from the heart, lung, and gizzard, no megalomeronts were seen in other organs of these three birds. The megalomeronts ranged from 175–369 μm (296.6 \pm 88.8, n = 4) in diameter and were all covered by a thick eosinophilic capsule-like wall. All megalomeronts were growing megalomeronts; no mature megalomeronts were observed. The megalomeronts detected in the two birds infected with the lineage hCCF5 were similar in morphology and characterized by the formation of irregularly shaped cytomeres (Fig. 8A-B, E-F, I-J). At high magnification, roundish subcytomeres with aggregating nuclei were identified (Fig. 8D, H, L). No host cell nuclei were seen in the investigated sections. A mild inflammatory reaction was present around one smaller megalomeront in the heart muscle but was absent around other megalomeronts.

The *H. majoris* megalomeront found in the gizzard of the third individual was morphologically different compared with the megalomeronts found in the individuals infected with hCCF5. This young megalomeront contained roundish to oval cytomeres which were patchily distributed throughout the megalomeront (Fig. 8M-O). Parasite nuclei were not recognizable. In the same bird, a second smaller megalomeront was found in the lung, but its lineage could not be identified due to it's absence in sections incubated with the *H. majoris*-specific probe (Supplementary Fig. S3).

3.5.5. Haemoproteus fringillae hCCF3 develops meronts exclusively in the lungs

Histological sections of three birds contained several small meronts of *H. fringillae* (Fig. 9). The meronts were exclusively found in the lungs and labelled by the hCCF3-specific probe, confirming they belonged to *H. fringillae*. Generally, meronts were scarce and randomly distributed across the lung sections. They showed elongate, wormlike forms and were $10.7 \pm 4.8 \, \mu m \, (n = 20)$ in size. Mer-



onts were filled with developing merozoites, indicating advanced maturity. In some of them, clefts were visible between groups of nuclei, suggesting cytomere formation (Fig. 9C). No inflammatory reactions were associated with meronts found in the lungs.

3.5.6. Haemoproteus exo-erythrocytic stages of unclear origin

A solitary Haemoproteus meront was found in the cardiac muscle (Fig. 10) of one bird infected with Haemoproteus spp. hCCF2, hROFI1, and Leucocytozoon sp. lBRAM3. No other meronts or megalomeronts were observed in additional sections investigated by H&E staining or ISH, preventing identification of the lineage. The meront was oval-shaped, 37 µm in diameter and located intracellularly. The infected host cell showed a hypertrophied nucleus, but the host cell type could not be determined. The developing parasite already showed signs of cytomere formation. No inflammatory reaction was seen around the infected cell.

4. Discussion

This study investigated natural haemosporidian co-infections in F. coelebs, a bird species common and widespread in the Western Palearctic (BirdLife International, https://www.birdlife.org, accessed April 5, 2023). Although haemosporidian infections have been studied quite extensively in F. coelebs both in the laboratory and the field (Valkiūnas, 2005), the present study is the first known one focusing on the exo-erythrocytic development of the parasites in this host species. It was challenging to approach this issue before the development of molecular diagnostic tools due to common coinfections with several distinct morphospecies and genetic lineages of haemoproteids, the exo-erythrocytic development of which was unknown. The main discoveries of this study are the development of meronts and megalomeronts of several Haemoproteus spp. commonly parasitizing F. coelebs, including H. magnus hCCF6, H. fringillae hCCF3, H. majoris hCCF5, Haemoproteus sp. hROFI1, and Haemoproteus sp. hCCF2, with the observation of merogonic stages in the vascular system, presenting a formerly unknown mode of exo-erythrocytic development in Haemoproteus parasites. The tissue stages of these species were distinct with respect to their morphology and organ distribution, indicating species-specific patterns of exo-erythrocytic development with different host tissue tropism. Furthermore, the study highlights that co-infections with different tissue stages of multiple parasites are frequent in F. coelebs and demonstrates how these can be untangled by targeting their tissue stages in naturally infected birds using laser microdissection and in situ hybridization, applying genus- and lineage-specific molecular probes.

The molecular results of this study are consistent with previous reports of high co-infection rates among F. coelebs (Valkiūnas et al., 2006; Mata et al., 2015) with Haemoproteus parasites dominating haemosporidian diversity (Ellis et al., 2020; Pellegrino et al., 2021). Additionally, this investigation showed that co-infections with more than two haemosporidian parasites are common but frequently missed during PCR screening using standard protocols. For example, the results from the nested PCR assay alone showed

one triple infection among the birds investigated, whereas combining the results with those obtained by additional techniques (LCM, ISH) revealed five triple infections. This adds to earlier sensitivity studies demonstrating that PCR diagnostics underestimate mixed infections in naturally infected birds (Valkiūnas et al., 2006) and emphasizes the need for better diagnostics and combinations of different techniques to obtain a more complete picture of parasite prevalence and diversity in certain host species.

All nine parasite lineages detected in this study were previously reported in F. coelebs, with some of the lineages being frequently recorded, including H. magnus hCCF6, Haemoproteus sp. hCCF2, H. majoris hCCF5, Haemoproteus sp. hCCF1, and H. fringillae hCCF3, with a prevalence ranging from 11% (hCCF3) to 35% (hCCF6), and most records originating from Morocco, Portugal, and Sweden (Drovetski et al., 2014; Ellis et al., 2020). Haemoproteus spp. are actively transmitted on the Curonian Spit. Lithuania (Valkiūnas. 2005) and expectedly, these lineages were also prevalent among the birds investigated in this study. In addition, Haemoproteus sp. hROFI1 was found in six (30%) birds, indicating that this lineage commonly infects F. coelebs. The lineage has also been previously recorded in this bird species, as well as in related Carduelis chloris and a few other finches (Drovetski et al., 2014; Nilsson et al., 2016; Ellis et al., 2020). Notably, in the present study, hROFI1 was missed during standard PCR screening in five of six birds and only detected by LCM and subsequent PCR using different primers. The reason for the lack of amplification using the first protocol might relate to the low abundance of parasite stages in the blood, as no or only a few ISH signals were detected in blood vessels, indicating low parasitaemia of hROFI1 in the birds investigated. In addition, preferential binding of the primers by Hellgren et al. (2004) to co-infecting lineages might have contributed to the low rate of amplification, particularly as both the forward and reverse primers showed three mismatches to the cytb sequence of hROFI1. This should be considered in future studies on F. coelebs and other fringillid species involving haemosporidian parasite screenings.

Based on the morphological analysis in this study, the lineages hCCF6 and hCCF09 were assigned to H. magnus, which is supported by their close phylogenetic relationship, differing by one bp in cvtb. While hCCF6 is very common in F. coelebs, hCCF09, detected in one bird by this study, appears to be very rare, as it was previously only recorded in three F. coelebs from Morocco and Portugal. Apart from F. coelebs, the lineage was found once in an Erithacus rubecula from Portugal, however this record might represent an accidental

The most striking findings of this study were the compartmented merogonic stages of Haemoproteus sp. hCCF2 observed in the lumen of several large blood vessels in the lungs, liver, and the skeletal muscle of infected birds (Fig. 6 and Supplementary Fig. S1). At first glance, the merogonic clusters appeared to be gigantic megalomeronts divided into multiple cytomeres, however, compared with megalomeronts of other Haemoproteus spp., the detected structures were clearly different in two features. First, a thick capsule-like wall typically covering big megalomeronts of Haemoproteus spp. (Valkiūnas and Iezhova, 2017) was lacking,

Fig. 6. Haemoproteus sp. hCCF2 meronts in the lung and the liver of Fringilla coelebs. In two birds, numerous meronts were found in the lumen of blood vessels in the lungs (A-H) and the liver (I-L) by H&E staining (A, C-E, G-I, K, L) and in situ hybridization (ISH) using a Haemoproteus genus-specific probe (B, F, J). The meronts formed compact clusters which occupied entire lumina of the vessels, the wall of which was labelled by immunohistochemistry using a marker for smooth muscle cell actin (B, F, J, white arrows, brown diaminobenzidine stain). The clusters displayed a unique arrangement of two types of meronts: young, poorly developed stages in the central core of the cluster (A-D, indicated by asterisks), and larger meronts more advanced in their development at the periphery (A, C-D, E, I, K, marked by black arrows). Note that poorly developed meronts stained bright eosinophilic and were unreactive to the ISH probe, whereas meronts more advanced in their development appeared more basophilic and showed intense ISH labelling. They were each covered by a thin membrane (D, L, indicated by short arrows). Note the mesh-like projections spanning an optically clear space around the meront (L, white arrowheads) and intermingling blood cells between neighbouring meronts. Sometimes vacuoles (D, K, L, indicated by open black triangles) were seen in developing meronts. Mature meronts contained numerous well differentiated merozoites (H, black arrowheads), which lacked ISH signal. Note the formation of a large thrombus (E, hash) blocking the vessel lumen and its channel-like connection (indicated by white open triangles) to the meront cluster. A moderate inflammatory reaction (indicated by white asterisks) was observed around affected vessels in the liver (I),, → meront; →, cytoplasmic membrane; ➤, merozoite; >, vacuoles; ★, young, undeveloped meronts; \implies , vessel wall; \gg , channel-like formation; *, inflammatory cells. Scale bars = 20 μ m.

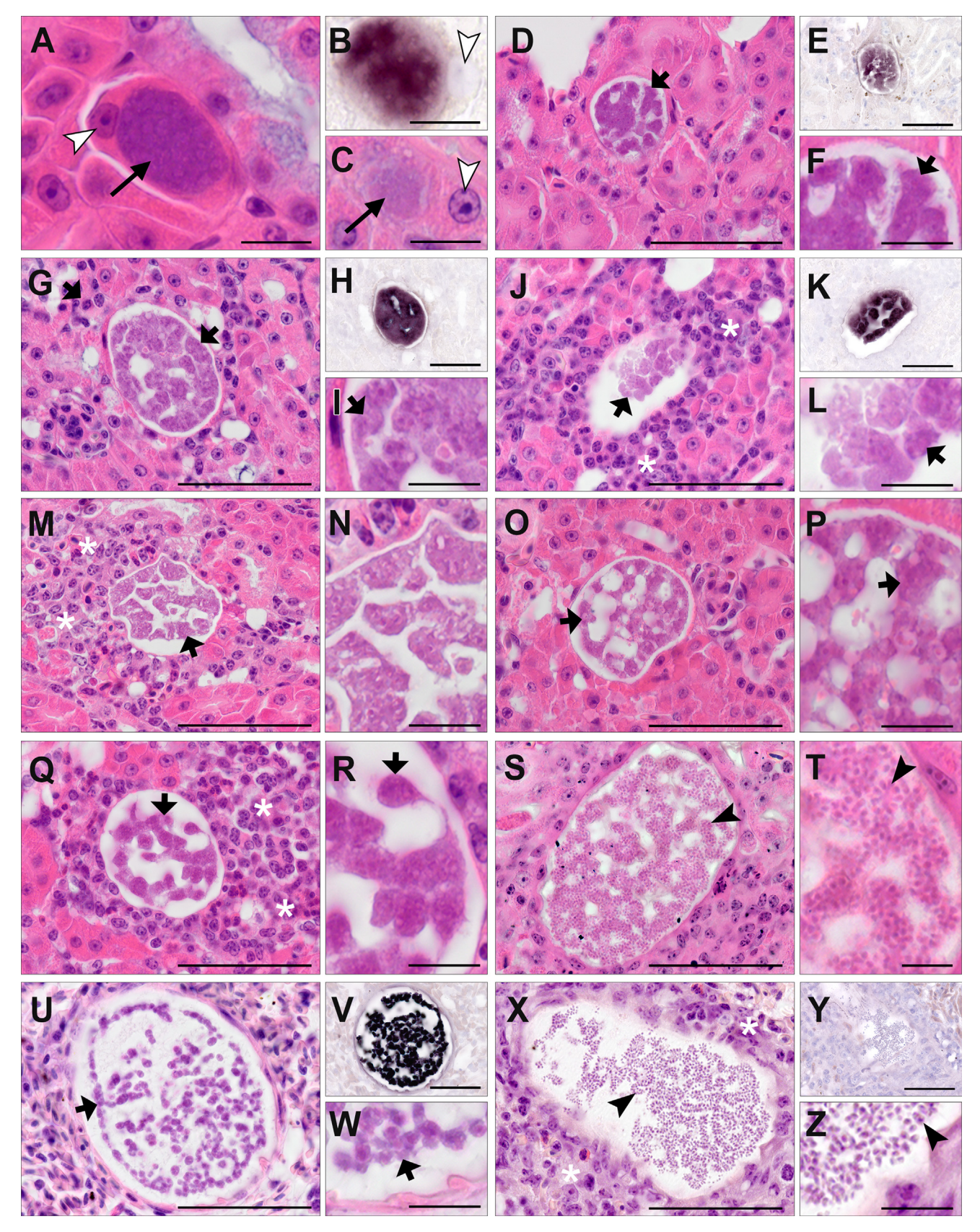


Fig. 7. Haemoproteus magnus hCCF6 megalomeronts in the kidneys (A-T) and lungs (U-Z) of Fringilla coelebs. Multiple megalomeronts were found in H&E-stained sections (A, C, D-G, I, J, L-U, W, X, Z) and identified by in situ hybridization (ISH) using a hCCF6-specific probe (B, E, H, K), and a Haemoproteus genus-specific probe (V, Y). Young meronts located in epithelial cells of renal tubules (A-C, arrows). Note the host cell nuclei (arrowheads) of the infected cells. Megalomeronts more advanced in their development showed varying degrees of cytomere formation (D-R, U-W, short black arrows). Nearly mature (S, T) and mature megalomeronts (X-Z) were filled with uninuclear merozoites (arrowheads) with cytomeres gradually disappearing. Note that a caspule-like wall typically covering Haemoproteus sp. megalomeronts was absent in all detected megalomeronts of H. magnus hCCF6. An inflammatory reaction (asterisks) was observed around most megalomeronts (J, M, Q, X). →, meront; →, cytomere; →, merozoite; ⊳, host cell nucleus; ∗, inflammatory cells. Scale bars = 10 μm (A-C, F, I, L, N, P, R, T, W, Z) and 50 μm (D, E, G, H, J, K, M, O, Q, S, U, V, X, Y).

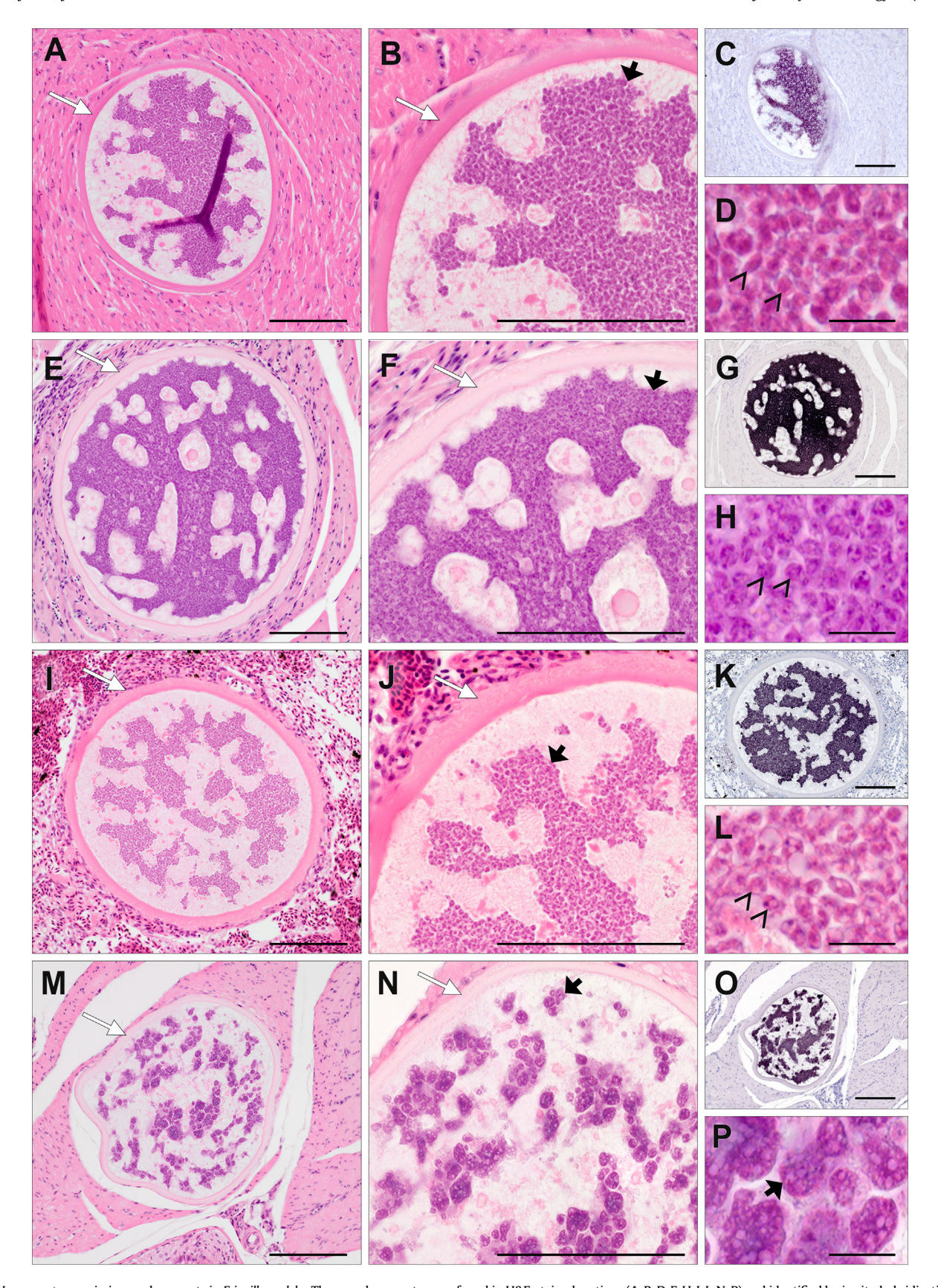


Fig. 8. Haemoproteus majoris megalomeronts in Fringilla coelebs. The megalomeronts were found in H&E-stained sections (A, B, D-F, H-J, L-N, P) and identified by in situ hybridization (ISH) using a H. majoris species-specific probe (C, G, K, O). Two birds infected with the lineage hCCF5 showed multiple megalomeronts in the heart muscle (A-H), and a single megalomeront in the lung (I-L). In another bird, a single H. majoris megalomeront was detected in the muscular layer of the gizzard (M-P), but its lineage was not identified. All megalomeronts were growing megalomeronts and covered by a thick eosinophilic wall (white arrows, A, B, E, F, I, J, M, N). Megalomeronts found in the H. majoris CCF5-infected birds (A-K) displayed similar morphology and cytomere formation (black arrows). At higher magnification, aggregation of nuclei in subcytomeres (indicated by open triangles) were seen (D, H, L). The H. majoris megalomeront found in the gizzard (M-P) differed in morphology but also showed cytomeres which were roundish and seemed vacuolated (black arrows, N, P). This megalomeront might belong to a different lineage of H. majoris. →, cytomeres; ➤, merozoite; >, subcytomere; ⇒, caspule-like wall. Scale bars = 100 μm (A-C, E-G, I-K, M-O) and 10 μm (D, H, L, P).

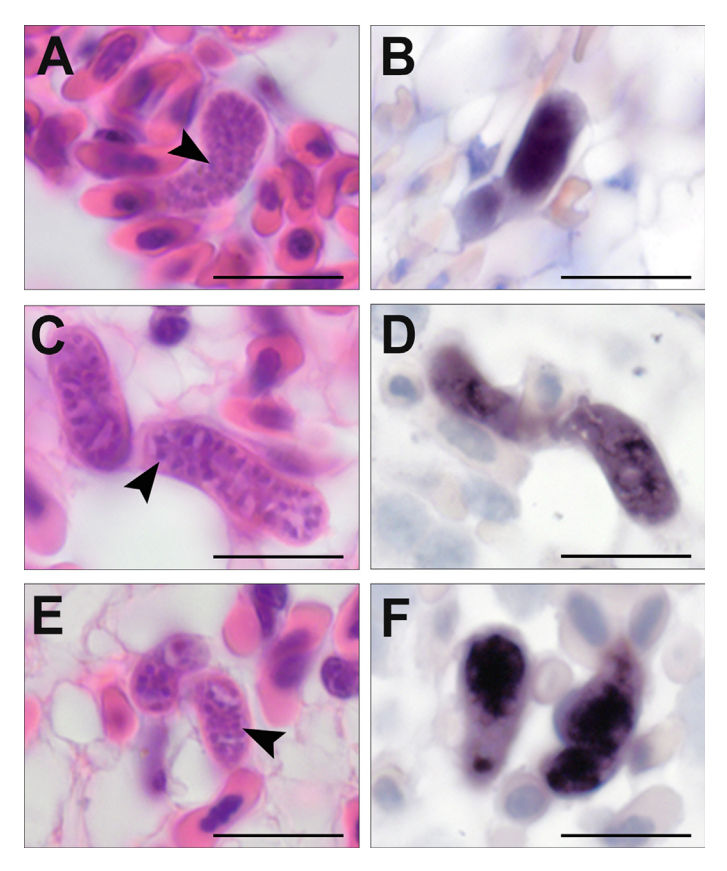


Fig. 9. Haemoproteus fringillae hCCF3 meronts in the lungs of Fringilla coelebs. Multiple meronts were detected in H&E-stained sections (A, C, E) of the lungs of three F. coelebs and identified by in situ hybridization (ISH) using a hCCF3 lineage-specific probe (B, D, F). The meronts were elongate, following the shape of capillaries and contained developing merozoites (arrowheads, A, C, E), indicating advanced maturation. Scale bars = 10 µm.

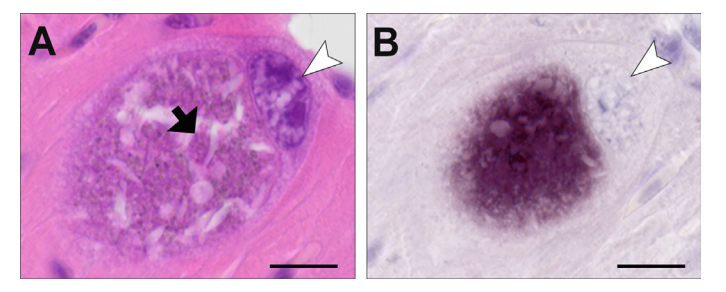


Fig. 10. Haemoproteus sp. meront in the heart of a *Fringilla coelebs* infected with *Haemoproteus* spp. hCCF2, hROFI1, and *Leucocytozoon* sp. lBRAM3. A solitary developing meront was detected in an H&E-stained section of the heart (A) and identified by in situ hybridization (ISH) using a *Haemoproteus* genus-specific probe (B). The meront located intracellularly and showed early cytomere formation (arrow). A hypertrophic host cell nucleus (arrowheads) was seen at the periphery of the infected cell. The lineage of this meront was not identified. Scale bars = 10 μm.

and second, the merogonic bodies constituting the clusters were each covered by a thin, eosinophilic membrane, suggesting that the various compartments represent individual multinucleated entities (meronts). Notably, host blood cells were observed between neighbouring compartments containing meronts with advanced differentiation (Fig. 6G, K, L), indicating that the merogonic clusters were not entirely enclosed at the observed stage of development. As the infected host cells or their nuclei were not distinguishable, it seems possible that these meronts developed extracellularly in the vascular lumen. As indicated above, the merogonic bodies of different clusters varied in maturity and differentiation, indicating asynchronous development across host tissues. Interestingly, within individual clusters, internal meronts appeared undifferentiated compared with meronts located at the periphery of the cluster. Internal meronts were also unreactive

during ISH, indicating low rRNA content. By contrast, meronts at the periphery were larger and strongly ISH-positive, indicating higher rRNA content, which could reflect ongoing protein synthesis required for parasite growth (Failmezger et al., 2017). Unfortunately, the progress of maturation and the mechanism of compartmentalization by which the meronts were formed and ultimately appeared in the circulation remain entirely unclear. Based on the observation of almost concentrically arranged undeveloped and differentiated meronts (Fig. 6A, B), and the fact that internal meronts adjoined closely with no visible space or host cells in between, it seems likely that the entire cluster developed in one piece rather than individual merogonic compartments becoming assembled in the circulation after their formation. In other words, the authors think that multiple merogonic compartments arise from the division of a single progenitor parasite stage, the origin of which

(sporozoite or merozoite) can only be speculated. Apicomplexan parasites demonstrate a variety of asexual division modes differing at the level of DNA replication and segregation, karyokinesis, and zoite assembly (budding) (Striepen et al., 2007; Gubbels et al., 2021). Species of the genera Plasmodium, Haemoproteus, and Leucocytozoon replicate via merogony, which involves multiple cycles of mitotic nuclear divisions resulting in a multinucleated stage (meront), followed by the formation of daughter cells (merozoites) which bud from the mother plasmalemma. It is conceivable that the observed individual meronts, each bounded by a thin membrane, represent separate cytomeres formed by multiple invaginations of the parasite plasma membranes during meront development, which were released into circulation after rupture of the host cell. Cytomere formation is commonly observed in Haemoproteus and Leucocytozoon exo-erythrocytic development (Valkiūnas, 2005; Valkiūnas and Jezhova, 2017), but the parasite membrane covering the intracellularly developing cytomeres is usually not discernible in light microscopic preparations, raising the question about the morphogenesis of such prominent parasite membranes of extracellularly developing meronts. Further electron microscopic studies and probably also immunocytochemical experiments are needed to elucidate the ultrastructural architecture of these compartmented meronts or cytomeres.

Regardless of the dividing mechanism by which the individual merogonic compartments (possible former cytomeres) were formed, it seems that they were released into the circulation at an early stage of development, either by active egression from the infected host cell or by its rupture. In the circulation, the early merogonic stages, contained in individual, membrane bounded compartments, could continue replication and differentiation extracellularly. Because meronts located at the periphery of such clusters face favouring conditions regarding nutrient uptake from the extracellular environment, they would develop first, whereas meronts located internally and deprived of the extracellular milieu might interrupt their cell cycle and develop later. This could explain the concentric appearance of undeveloped and differentiated meronts within individual clusters and corresponding differences in ISH probe reactivity. Further, maturation of the individual merogonic stages might be accompanied by alterations in plasma membrane stability and connectivity, which could explain the appearance of host blood cells between compartments containing meronts which were more advanced in their development. Eventually, mature meronts would detach completely from the cluster, or rupture and release merozoites, as seen in one of the clusters in a pulmonary artery. Mature merozoites lacked ISH signal, a phenomenon which has been observed in other haemosporidian parasites (Duc et al., 2023b) and might reflect the ceasing of ribosome biogenesis in fully developed merozoites. These merozoites could ultimately infect erythrocytes and develop into gametocytes.

Notably, clusters of compartmented meronts as observed in this study are not unique to the Haemoproteus parasites described herein. Similar merogonic stages have been reported in sparrows infected with Haemoproteus passeris (Paperna and Gill, 2003; Valkiūnas and Iezhova, 2017). In particular, the exo-erythrocytic stages reported by Paperna and Gill (2003) resemble the merogonic stages of Haemoproteus sp. hCCF2. Interestingly, exoerythrocytic stages of *H. passeris* were also observed in the lungs and liver of the infected sparrows, and although it was not specifically mentioned, these stages seemed to locate in blood vessels too, based on the published photographs. These findings suggest similarities in the merogonic development of H. passeris and Haemoproteus sp. hCCF2, which seems reasonable considering their close phylogenetic relationship, differing by 13 bp or 2.7% in the cytb barcode. However, despite overall similar morphology and site of development of the two parasites, some differences were noted

between their exo-erythrocytic stages. For example, the concentric arrangement of undeveloped and differentiated meronts in clusters of hCCF2 was not reported in compartmented meronts of *H. passeris*, where development was highly asynchronous across meronts. On the other hand, the formation of cytomeres with peripheral merozoite assembly reported in *H. passeris* was not seen in stages of *Haemoproteus* sp. CCF2, albeit this might be because not all sequential stages of the differentiation process were present in the samples examined. Also, solitary multinucleated merogonic bodies, as reported in sparrows infected with *H. passeris*, were absent in *F. coelebs* investigated here. However, Paperna and Gill (2003) speculated, that solitary merogonic bodies might have detached from meront assemblies rather than presenting initial stages, thus this feature might not present a strong character.

Apart from H. passeris, merogonic stages visually similar to those of Haemoproteus sp. hCCF2 have been observed during megalomerogony of Leucocytozoon caullervi (Isobe and Akiba, 1990: Hae et al., 2016; Sawale et al., 2018; Pohuang et al., 2021), a pathogenic parasite which belongs to the Leucocytozoon subgenus Akiba and parasitizes domestic chicken in southeastern Asia (Fallis et al., 1974; Valkiūnas, 2005; Nakamura, 2022). Megalomeronts of this parasite originate from second generation merogony in endothelial cells, which rupture and release developing cytomeres. Subsequently, these stages spread into various organs, were they finish maturation extracellularly (Isobe and Akiba, 1990; Valkiūnas and Iezhova, 2017). The histological appearance of these megalomeronts resembles the compartmented stages of Haemoproteus sp. CCF2 in that they also display an optically clear space between the meront and its bounding membrane. These empty spaces might have been filled with cytoplasmic fluids that were washed out during tissue processing. However, opposed to the hCCF2 meronts which exclusively appeared in clusters, L. caulleryi megalomeronts were also seen as solitary bodies, reaching relatively large sizes (more than 300 µm). When occurring in groups, they were usually smaller and interspersed in the tissues of organs, but never reported within the lumen of blood vessels. It is important to note that L. caulleryi has a unique position among Leucocytozoon parasites. Unlike parasites of the subgenus Leucocytozoon, which are transmitted by black flies (Simuliidae), L. caulleryi is transmitted by biting midges of the genus Culicoides (Ceratopogonidae), as are parasites of the Haemoproteus subgenus Parahaemoproteus (Morii, 1992; Valkiūnas, 2005). Phylogenetic studies also suggested a closer relationship of *L. caulleryi* with *Parahaemoproteus* parasites than with members of the subgenus Leucocytozoon (Pacheco et al., 2018). From this point of view, it seems unsurprising to find similarities in morphology and development of their exo-erythrocytic stages, but the mechanism of their dispersal and location in the organs might be different. It is noteworthy that, apart from L. caulleryi, an intravascular mode of meront development has so far only been reported in another Leucocytozoon parasite, Leucocytozoon (subgenus Leucocytozoon) sp. ISTAL5 infecting owls (Ilgūnas et al., 2022). The discovery of meronts of *Haemoproteus* parasites in the blood circulation in the present study demonstrates that intravascular development occurs in parasites of both genera. Further studies, preferably experimental, are needed to elucidate the underlying mechanism of merogony responsible for the peculiar morphology and extracellular appearance of these parasite stages, as well as the morphogenesis of their bounding membranes.

The meront clusters of hCCF2 clearly induced an immune reaction by the host, as evident from inflammatory cell infiltrations around affected vessels and the formation of foreign body giant cells. Due to the sizes of the meront clusters, they also likely caused occlusion of the vessels, resulting in local haemostasis and thrombosis as seen in one of the pulmonary arteries. Whether these lesions were sufficient to cause systemic clinical signs in the infected birds remains questionable, however they suggest detri-

mental effects of haemoproteosis due to infection with *Haemoproteus* sp. CCF2.

The second most important finding of this investigation was the location of meronts of Haemoproteus sp. hROFI1 in the brain of several birds. Merogony in brain tissue is commonly observed during avian malaria (Huff, 1957; Dinhopl et al., 2015; Ilgūnas et al., 2016; Himmel et al., 2020), and hence is characteristic for many parasite species of the genus Plasmodium. So far, exo-erythrocytic stages of Haemoproteus parasites in the brain of infected hosts have only been reported recently, referring to large megalomeronts formed by the parasites (Duc et al., 2021). The Haemoproteus meronts observed in this study very much resembled Plasmodium phanerozoites typically developing in endothelial cells of capillaries, except for the conspicuous cytomeres (see Fig. 5F, J, K, L, O), which seem absent in meronts of avian malaria parasites. Immunohistochemical staining showed that hROFI1 meronts also developed in brain endothelial cells, suggesting a similar infection pattern. However, while meronts of *Plasmodium* parasites often display an even distribution across brain sections, (see for example in Dinhopl et al. 2011; Himmel et al., 2020), hROFI1 meronts showed rather a multifocal distribution and frequently clustered tightly in groups (Fig. 5G-L). Individual meronts often developed in neighbouring endothelial cells which, depending on the course of the capillary, typically results in cross-sections of one or several meronts in a row. The unusual appearance of clustering meronts randomly adjoining one another could result from the cross-section through a small, convoluted microcapillary network formed at this site. However, while the brain is highly vascularized, exhibiting a hierarchical organization of arterioles and venules branching into and converging from a dense network of capillaries (Smith et al., 2019), the existence of such convoluted formations within the capillary bed is undocumented, suggesting they could represent vascular malformations, possibly induced by the parasitic infection. This is a completely new aspect of pathology during haemoproteosis and requires careful attention during future examinations to explore whether these findings were incidental or present manifestations of the disease. Certainly, the presence of replicating parasites triggered a local inflammatory response driven by mononuclear cells, as evident by perivascular infiltration and gliosis accompanying invaded endothelia. However, the role of multinucleated giant cells in phagocytosis of parasite stages, as occasionally observed, remains questionable.

Interestingly, merogony of hROFI1 was restricted to cerebral endothelial cells but not observed in endothelia of other organs examined, suggesting strong tissue tropism towards the brain, characteristic of Haemoproteus sp. hROFI1. In this regard, exoerythrocytic merogony is distinct from avian Plasmodium parasites, which invade endothelia of diverse organs (Valkiūnas, 2005). Endothelial cells display a large phenotypic heterogenicity between different tissues and organs, and cerebral endothelial cells are characterized by unique cellular and molecular properties, which distinguish them from endothelia in other organs (Ross et al., 2020). It thus can be assumed that certain attributes of brain endothelial cells are implicated in cell recognition and invasion by the parasite, however this aspect of host-parasite interaction is largely unexplored in avian haemosporidian parasites. It is important to note that it was impossible to determine the time of infection in the birds, leaving open the question of whether merogony would be restricted to the brain in all phases of exo-erythrocytic development of this parasite. Due to the unknown timing of infection, it also remains unclear whether the observed meronts were formed during primary merogony or present second generation meronts. ISH with the hROFI1-specific probe revealed only a few blood stage signals in three of six birds infected with this lineage, suggesting low parasitaemia in these cases, whereas exo-erythrocytic stages were found in all of them. These results could indicate ongoing pre-erythrocytic merogony of the parasites in the birds examined, or an early erythrocytic phase of infection, with just a few blood cells infected. Unfortunately, due to the presence of co-infecting *Haemoproteus* spp., and missing morphological characterization of hROFI1 gametocytes, these assumptions could not be confirmed by blood film evaluation, calling for further studies including morphological description of this lineage.

Similar to Haemoproteus sp. hROFI1 replicating exclusively in brain tissue, merogony of H. fringillae hCCF3 was restricted to the lungs of infected birds, suggesting a comparable degree of host tissue tropism, although the involved host cell type might be different. While exo-erythrocytic merogony in the lungs has been described in diverse Haemoproteus spp. (Baker, 1966; Peirce, 1976; Sibley and Werner, 1984; Garvin et al., 2003; Valkiūnas, 2005; Hernández-Lara et al., 2021), most of them were also observed to form meronts in other organs, indicating that narrow tissue tropism could be characteristic of H. fringillae. However. due to the scarcity of meronts in the investigated birds and the low bird sample size, the examination of additional individuals is required to confirm these observations. Morphologically, H. fringillae meronts were small and hardly distinguishable from meronts of diverse Plasmodium spp. developing in the lungs (compare for example with Alley et al., 2008; Dinhopl et al., 2011; Howe et al., 2012; Ilgūnas et al., 2016; Himmel et al., 2020; Pendl et al., 2022), and presumably also other species of Haemoproteus described in older literature (see Valkiūnas, 2005). Without the application of genus- and lineage-specific probes, the taxonomic assignment of the detected meronts would have been impossible, demonstrating that specific molecular probes are invaluable tools for the identification of haemosporidian tissue stages and study of their developmental patterns.

Species- and lineage-specific probes were also used to identify megalomeronts of hCCF5 and hCCF6, extending the list of Haemoproteus lineages for which megalomeronts have been reported to date. The lineage hCCF5 has been linked to H. majoris recently, reporting megalomeronts in various tissues (Duc et al., 2023a). The lineage hCCF6 was linked to H. magnus in this study, and exo-erythrocytic stages of this species were described for the first known time. They were distinguishable from megalomeronts of other Haemoproteus spp. by pronounced cytomere formation resulting in numerous well-delimited round cytomeres observed in late stages of development. The most distinct feature, however, was the lack of a capsular-like wall around megalomeronts. Clearly, the development of megalomeronts started intracellularly, evident from early stages detected in renal tubule cells. By contrast, stages more advanced in development were not attributable to infected host cells, raising the question whether they continued maturation extracellularly. Nevertheless, the parasite seemed to develop within the confines of its plasma membrane, as most developing stages were well delimited from the surrounding host tissue. Notably, the megalomeronts induced local inflammation, indicating a marked immune response which might be explained by the lack of a protective wall, similar to disrupted megalomeronts of Haemoproteus spp. reported in previous studies (Atkinson et al., 1988; Donovan et al., 2008; Duc et al., 2021). Megalomeronts of hCCF6 were found exclusively in lungs and kidneys of the infected birds, suggesting a preferred site for exoerythrocytic development. As for the hROFI1 and hCCF3 meronts restricted to the brain and lungs, respectively, the cellular or molecular mechanism underlying the tissue-specific merogonic development of H. magnus hCCF6 remains elusive.

Host tissue tropism was less obvious in exo-erythrocytic stages of *H. majoris* hCCF5, as megalomeronts were found in the lungs, heart muscle, and gizzard of infected birds, albeit not in all these organs within the same individuals. The morphology of megalomeronts of hCCF5 described in this study is comparable to megalomeronts.

eronts of other lineages belonging to *Haemoproteus majoris* (hPARUS1, hPHYBOR04, and hPHSIB1), supporting the idea of similar merogonic development among closely related lineages and the taxonomic value of this character (Ilgūnas et al., 2019a, 2019b; Duc et al., 2020, Duc et al., 2023a). Notably, the solitary *H. majoris* megalomeront found in the gizzard of one of the birds differed from the hCCF5 megalomeronts in the other individuals by the appearance of round cytomeres, which were less interconnected but well separated (Fig. 8M). While the lineage of this megalomeront remained unidentified, it most likely belongs to another lineage of *H. majoris*, as it was labelled by the *H. majoris* specific probe. Further studies including other *H. majoris* lineages are necessary to explore intraspecific variation of megalomeront morphology in this parasite species.

In line with earlier descriptions of Haemoproteus tissue stages (see in Valkiūnas, 2005), the study showed that Haemoproteus parasites vary markedly in their exo-erythrocytic stages with regard to their morphology, location and distribution. An intriguing question has been whether these variations present phylogenetically informative parasite traits or reflect phenotypic adaptations mediated, for example, by different host-parasite associations. In particular, the origin of large megalomeronts regularly reported in different bird hosts and often causing severe pathologies (Atkinson and Forrester, 1987; Borst and Zwart, 1972; Cardona et al., 2002; Lederer et al., 2002; Peirce et al., 2004; Pennycott et al., 2006; Stidworthy and Greenwood, 2006; Ferrell et al., 2007; Baker et al., 2018; Niedringhaus et al., 2018), has been unclear on many occasions, leaving questions about which species develop megalomeronts, and whether these form during regular development or result from aberrant infections in "wrong" hosts. The application of DNA barcoding in recent morphological studies brought light to this issue, demonstrating that megalomeronts are formed during natural development in certain Haemoproteus spp. (Groff et al., 2019; Ilgūnas et al., 2019a, 2019b; Duc et al., 2020; Himmel et al., 2020). This is corroborated by the observation of Haemoproteus spp. megalomeronts in naturally infected F. coelebs investigated in this study. Interestingly, phylogenetic reconstruction including all Haemoproteus spp. for which reported tissue stages have been supported by molecular data, placed nonmegalomeront-forming species into one big clade, whereas species known to form megalomeronts appeared in different clades across the tree, suggesting phylogenetic divergence. However, the clades obtained only low support and due to the polytomies in the tree, it is difficult to draw conclusions about the phylogenetic character of this trait based on the available data. Analyses of whole mitochondrial genomes or multiple nuclear genes likely would allow resolution of the phylogenetic relationships between nonmegalomeront- and megalomeront-forming parasites.

Concerning the question about which haemosporidian species form either type of meronts, the application of species- and lineage-specific probes proved very helpful in assigning detected tissue stages to co-infecting parasite species. This is the first known study which applied this methodology in research of exoerythrocytic development in wildlife haemosporidian parasites. However, the present investigation also demonstrated limitations of this approach, particularly in cases of rare tissue stages. Small meronts or early developing megalomeronts might not be present in subsequent tissue sections and thus unavailable for further ISHbased testing. For example, the solitary Haemoproteus meront found in the cardiac muscle of one bird was not present in additional sections prepared, preventing species identification. The bird was infected with the Haemoproteus lineages hCCF2 and hROFI1, however, considering the location and morphology of hCCF2 and hROFI1 tissue stages found in other birds, it seemed unlikely that the meront found in the heart belonged to one of these lineages,

suggesting the presence of another undetected *Haemoproteus* sp. in this sample.

In the absence of prior knowledge about the parasite lineages possibly involved in an infection, or missing 18S ribosomal gene sequences of species for the design of specific probes, laser microdissections can aid identification of tissue stages, as was the case in *Haemoproteus* sp. hCCF2 meronts. However, this approach requires adequate fixation of tissue samples to preserve good DNA quality for PCR-based analysis. Specifically, prolonged formalin fixation leads to fragmentation of DNA due to protein crosslinking, diminishing success of amplification. This was likely the reason for unsuccessful PCRs in case of meronts dissected from brain sections of the two birds obtained in 2019, as these samples were stored in formalin for an extended period of several weeks. Ideally, for future morphological studies focusing on exoerythrocytic stages of haemosporidian parasites, tissue fixation should be standardized and not exceed 24 h.

In conclusion, the combination of different methods for lineageand species-specific identification of tissue stages revealed different host tissue tropism among co-infecting Haemoproteus spp. in F. coelebs, ranging from highly selective species colonizing single organs to less specialized parasite species exploiting as much as three different tissues. In addition, Haemoproteus sp. hCCF2 was found in the vascular system, presenting an untypical extracellular environment and mode of exo-erythrocytic development for obligatory intracellular parasites, and providing the first known evidence for intravascular development in parasites of the genus Haemoproteus. Given that all these lineages occur in sympatry and are highly prevalent in F. coelebs, it could be hypothesized that different tissue tropism of Haemoproteus spp. resulted from interspecific competition between parasites co-infecting the same host, leading to exploitation of different niches within the host's body for asexual replication. Being beneficial for different parasites, however, this also might result in pathology and damage of different organs, increasing the pathological effect of co-infections on hosts. Further systematic studies focusing on the exoervthrocytic development of the parasites not only in F. coelebs, but also other bird species commonly parasitized by multiple haemosporidian species, are needed to explore this hypothesis and better understand haemosporidian exo-erythrocytic merogony and distribution in avian hosts.

Declaration of Competing Interest

The authors declare that they have no known competing financial interests or personal relationships that could have appeared to influence the work reported in this paper.

Acknowledgements

We thank Melanie Stargardt from the VetCore Facility for Research, Vetmeduni Vienna, Austria, for her assistance with laser microdissection. Further, we thank Carolina R. F. Chagas and Mélanie Duc from the P. B. Šivickis Laboratory of Parasitology, Nature Research Centre Vilnius, Lithuania for assistance during fieldwork. This study complies with the current law of Lithuania. It was performed by licenced researchers and approved by the Environmental Protection Agency, Lithuania (permits 2018-04-13, no. 24; 2019-04-19, no. 23; 2020-04-07, no. 21; 2021-05-05, no. 26-SR-96). This research was funded in whole, or in part, by the Austrian Science Fund (FWF) (grant P 33480). For the purpose of open access, the author has applied a CC BY public copyright licence to any Author Accepted Manuscript version arising from this submission.

Appendix A. Supplementary data

Supplementary data to this article can be found online at https://doi.org/10.1016/j.jipara.2023.07.004.

References

- Alarcon-Martinez, L., Yilmaz-Ozcan, S., Yemisci, M., Schallek, J., Kılıç, K., Can, A., Di Polo, A., Dalkara, T., 2018. Capillary pericytes express α-smooth muscle actin, which requires prevention of filamentous-actin depolymerization for detection. Elife 7, 1–17. https://doi.org/10.7554/eLife.34861.
- Alley, M., Fairley, R., Martin, D., Howe, L., Atkinson, T., 2008. An outbreak of avian malaria in captive yellowheads/mohua (Mohoua ochrocephala). N. Z. Vet. J. 56, 247–251. https://doi.org/10.1080/00480169.2008.36842.
- Asghar, M., Hasselquist, D., Hansson, B., Zehtindjiev, P., Westerdahl, H., Bensch, S., 2015. Hidden costs of infection: chronic malaria accelerates telomere degradation and senescence in wild birds. Science 1979 (347), 436–438. https://doi.org/10.1126/science.1261121.
- Atkinson, C.T., Forrester, D.J., 1987. Myopathy associated with megaloschizonts of Haemoproteus meleagridis in a wild turkey from Florida. J. Wildl. Dis. 23, 495–498. https://doi.org/10.7589/0090-3558-23.3.495.
- Atkinson, C.T., Forrester, D.J., Greiner, E.C., 1988. Pathogenicity of Haemoproteus meleagridis (Haemosporina: Haemoproteidae) in Experimentally Infected Domestic Turkeys. J. Parasitol. 74, 228. https://doi.org/10.2307/3282448.
- Atkinson, C.T., Van Riper III, C., 1991. Pathogenicity and epizootiology of avian haematozoa: plasmodium, Leucocytozoon, and Haemoproteus. In: Loye, J.E., Zuk, M. (Eds.), Bird-Parasite Interactions. Oxford University Press, Oxford, UK, pp. 19–48.
- Baker, J.R., 1966. Haemoproteus palumbis sp. nov. (Sporozoa, Haemosporina) of the English Wood-Pigeon Columba p. palumbus. J. Protozool. 13, 515–519. https://doi.org/10.1111/j.1550-7408.1966.tb01954.x.
- Baker, K.C., Rettenmund, C.L., Sander, S.J., Rivas, A.E., Green, K.C., Mangus, L., Bronson, E., 2018. Clinical Effect of Hemoparasite Infections in Snowy Owls (Bubo scandicus). J. Zoo Wildl. Med. 49, 143–152. https://doi.org/10.1638/2017-0042R.1.
- Bennett, G.F., Peirce, M.A., Ashford, R.W., 1993. Avian Haematozoa: mortality and pathogenicity. J. Nat. Hist. 27, 993–1001. https://doi.org/10.1080/00222939300770621.
- Bennett, G.F., Peirce, M.A., Earlé, R.A., 1994. An annotated checklist of the valid avian species of Haemoproteus, Leucocytozoon (Apicomplexa: Haemosporida) and Hepatozoon (Apicomplexa: Haemogregarinidae). Syst. Parasitol. 29, 61–73. https://doi.org/10.1007/BF00009839.
- Bensch, S., Hellgren, O., Pérez-Tris, J., 2009. MalAvi: a public database of malaria parasites and related haemosporidians in avian hosts based on mitochondrial cytochrome b lineages. Mol. Ecol. Resour. 9, 1353–1358. https://doi.org/10.1111/j.1755-0998.2009.02692.x.
- Bernotienė, R., Palinauskas, V., Iezhova, T., Murauskaitė, D., Valkiūnas, G., 2016. Avian haemosporidian parasites (Haemosporida): a comparative analysis of different polymerase chain reaction assays in detection of mixed infections. Exp. Parasitol. 163, 31–37. https://doi.org/10.1016/j.exppara.2016.01.009.
- Borst, G.H.A., Zwart, P., 1972. An aberrant form of Leucocytozoon infection in two quaker parakeets (Myiopsitta monachus Boddaert, 1783). Z. Parasitenkd. 40, 131–138. https://doi.org/10.1007/BF00329148.
- Cardona, C.J., Ihejirika, A., McClellan, L., 2002. *Haemoproteus lophortyx* infection in Bobwhite quail. Avian Dis. 46, 249–255. https://doi.org/10.1637/0005-2086 (2002)046[0249:hliibq]2.0.co;2.
- Clark, N.J., Clegg, S.M., Lima, M.R., 2014. A review of global diversity in avian haemosporidians (Plasmodium and Haemoproteus: Haemosporida): new insights from molecular data. Int. J. Parasitol. 44, 329–338. https://doi.org/ 10.1016/j.ijpara.2014.01.004.
- Dimitrov, D., Zehtindjiev, P., Bensch, S., 2010. Genetic diversity of avian blood parasites in SE Europe: cytochrome b lineages of the genera Plasmodium and Haemoproteus (Haemosporida) from Bulgaria. Acta Parasitol. 55, 201–209. https://doi.org/10.2478/s11686-010-0029-z.
- Dinhopl, N., Mostegl, M.M., Richter, B., Nedorost, N., Maderner, A., Fragner, K., Weissenböck, H., 2011. Application of *in-situ* hybridization for the detection and identification of avian malaria parasites in paraffin wax-embedded tissues from captive penguins. Avian Pathol. 40, 315–320. https://doi.org/10.1080/03079457.2011.569533.
- Dinhopl, N., Nedorost, N., Mostegl, M.M., Weissenbacher-Lang, C., Weissenböck, H., 2015. *In situ* hybridization and sequence analysis reveal an association of *Plasmodium* spp. with mortalities in wild passerine birds in Austria. Parasitol. Res. 114, 1455–1462. https://doi.org/10.1007/s00436-015-4328-z.
- Donovan, T.A., Schrenzel, M., Tucker, T.A., Pessier, A.P., Stalis, I.H., 2008. Hepatic hemorrhage, hemocoelom, and sudden death due to *Haemoproteus* infection in passerine birds: eleven cases. J. Vet. Diagn. Invest. 20, 304–313. https://doi.org/ 10.1177/104063870802000307.
- Drovetski, S.V., Aghayan, S.A., Mata, V.A., Lopes, R.J., Mode, N.A., Harvey, J.A., Voelker, G., 2014. Does the niche breadth or trade-off hypothesis explain the abundance-occupancy relationship in avian Haemosporidia? Mol. Ecol. 23, 3322–3329. https://doi.org/10.1111/mec.12744.

- Duc, M., Ilgūnas, M., Valkiūnas, G., 2020. Patterns of Haemoproteus majoris (Haemosporida, Haemoproteidae) megalomeront development. Acta Trop. 212, https://doi.org/10.1016/j.actatropica.2020.105706 105706.
- Duc, M., Ilgūnas, M., Kubiliūnaitė, M., Valkiūnas, G., 2021. First report of Haemoproteus (Haemosporida, Haemoproteidae) megalomeronts in the brain of an avian host, with description of megalomerogony of Haemoproteus pastoris, the blood parasite of the common starling. Animals 11, 2824. https://doi.org/10.3390/ani11102824.
- Duc, M., Himmel, T., Harl, J., lezhova, T., Nedorost, N., Matt, J., Ilgūnas, M., Weissenböck, H., Valkiūnas, G., 2023a. Comparative analysis of the exoerythrocytic development of five lineages of *Haemoproteus majoris*, a common haemosporidian parasite of European passeriform birds. Pathogens 12, 898. https://doi.org/10.3390/pathogens12070898.
- Duc, M., Himmel, T., Ilgūnas, M., Eigirdas, V., Weissenböck, H., Valkiūnas, G., 2023b. Exo-erythrocytic development of two Haemoproteus species (Haemosporida, Haemoproteidae), with description of Haemoproteus dumbbellus, a new blood parasite of bunting birds (Emberizidae). Int. J. Parasitol.
- Ellis, V.A., Huang, X., Westerdahl, H., Jönsson, J., Hasselquist, D., Neto, J.M., Nilsson, J.Á., Nilsson, J., Hegemann, A., Hellgren, O., Bensch, S., 2020. Explaining prevalence, diversity and host specificity in a community of avian haemosporidian parasites. Oikos 129, 1314–1329. https://doi.org/10.1111/oik.07280.
- Failmezger, J., Ludwig, J., Nieß, A., Siemann-Herzberg, M., 2017. Quantifying ribosome dynamics in *Escherichia coli* using fluorescence. FEMS Microbiol. Lett. 364, fnx055. https://doi.org/10.1093/femsle/fnx055.
- Fallis, A.M., Desser, S.S., Khan, R.A., 1974. On species of Leucocytozoon. Adv. Parasitol. 12, 1–67. https://doi.org/10.1016/S0065-308X(08)60386-3.
- Fallon, S.M., Ricklefs, R.E., 2008. Parasitemia in PCR-detected *Plasmodium* and *Haemoproteus* infections in birds. J. Avian Biol. 39, 514–522. https://doi.org/10.1111/j.0908-8857.2008.04308.x.
- Fecchio, A., Chagas, C.R.F., Bell, J.A., Kirchgatter, K., 2020. Evolutionary ecology, taxonomy, and systematics of avian malaria and related parasites. Acta Trop. 204, https://doi.org/10.1016/j.actatropica.2020.105364 105364.
- Ferrell, S.T., Snowden, K., Marlar, A.B., Garner, M., Lung, N.P., 2007. Fatal hemoprotozoal infections in multiple avian species in a zoological park. J. Zoo Wildl. Med. 38, 309–316. https://doi.org/10.1638/1042-7260(2007)038[0309: FHIIMA]2.0.CO;2.
- Garvin, M.C., Homer, B.L., Greiner, E.C., 2003. Pathogenicity of Haemoproteus danilewskyi, Kruse, 1890, in blue jays (Cyanocitta cristata). J. Wildl. Dis. 39, 161–169. https://doi.org/10.7589/0090-3558-39.1.161.
- Groff, T.C., Lorenz, T.J., Crespo, R., lezhova, T., Valkiūnas, G., Sehgal, R.N.M., 2019. Haemoproteosis lethality in a woodpecker, with molecular and morphological characterization of Haemoproteus velans (Haemosporida, Haemoproteidae). Int. J. Parasitol Parasites Wildl 10, 93–100. https://doi.org/10.1016/j. ijppaw.2019.07.007.
- Gubbels, M., Coppens, I., Zarringhalam, K., Duraisingh, M.T., Engelberg, K., 2021. The modular circuitry of apicomplexan cell division plasticity. Front. Cell. Infect. Microbiol. 11, 1–17. https://doi.org/10.3389/fcimb.2021.670049.
- Hae, R., Bon-Sang, K., Eun-Ok, J., Moo-Sung, H., Kyung-Cheol, M., Seung, B., Yeonji, B., In-Pil, M., 2016. Pathology and molecular characterization of recent Leucocytozoon caulleryi cases in layer flocks. J. Biomed. Res. 30, 517. https://doi.org/10.7555/JBR.30.2016K0017.
- Hall, T.A., 1999. BioEdit: a user-friendly biological sequences alignment editor and analysis program for Windows 95/98/NT. Nucleic Acids Symp. Ser. 41, 95–98.
- Harl, J., Himmel, T., Ilgūnas, M., Valkiūnas, G., Weissenböck, H., 2023. The 18S rRNA genes of Haemoproteus (Haemosporida, Apicomplexa) parasites from European songbirds with remarks on improved parasite diagnostics. Malar. J. 22, 232. https://doi.org/10.1186/s12936-023-04661-9.
- Harl, J., Himmel, T., Valkiūnas, G., Weissenböck, H., 2019. The nuclear 18S ribosomal DNAs of avian haemosporidian parasites. Malar. J. 18, 305. https://doi.org/ 10.1186/s12936-019-2940-6.
- Hellgren, O., Waldenström, J., Bensch, S., 2004. A new PCR assay for simultaneous studies of *Leucocytozoon*, *Plasmodium*, and *Haemoproteus* from avian blood. J. Parasitol. 90, 797–802. https://doi.org/10.1645/GE-184R1.
- Hellgren, O., Pérez-Tris, J., Bensch, S., 2009. A jack-of-all-trades and still a master of some: prevalence and host range in avian malaria and related blood parasites. Ecology 90, 2840–2849. https://doi.org/10.1890/08-1059.1.
- Hernández-Lara, C., Duc, M., Ilgūnas, M., Valkiūnas, G., 2021. Massive infection of lungs with exo-erythrocytic meronts in European robin *Erithacus rubecula* during natural *Haemoproteus attenuatus* haemoproteosis. Animals 11, 3273. https://doi.org/10.3390/ani11113273.
- Himmel, T., Harl, J., Kübber-Heiss, A., Konicek, C., Fernández, N., Juan-Sallés, C., Ilgūnas, M., Valkiūnas, G., Weissenböck, H., 2019. Molecular probes for the identification of avian *Haemoproteus* and *Leucocytozoon* parasites in tissue sections by chromogenic in situ hybridization. Parasit. Vectors 12, 282. https://doi.org/10.1186/s13071-019-3536-2.
- Himmel, T., Harl, J., Pfanner, S., Nedorost, N., Nowotny, N., Weissenböck, H., 2020. Haemosporidioses in wild Eurasian blackbirds (Turdus merula) and song thrushes (T. philomelos): an in situ hybridization study with emphasis on exo-erythrocytic parasite burden. Malar. J. 19, 69. https://doi.org/10.1186/ s12936-020-3147-6.
- Himmel, T., Harl, J., Matt, J., Weissenböck, H., 2021. A citizen science-based survey of avian mortality focusing on haemosporidian infections in wild passerine birds. Malar. J. 20, 417. https://doi.org/10.1186/s12936-021-03949-y.
- Howe, L., Castro, I.C., Schoener, E.R., Hunter, S., Barraclough, R.K., Alley, M.R., 2012.Malaria parasites (Plasmodium spp.) infecting introduced, native and endemic

- New Zealand birds. Parasitol. Res. 110, 913–923. https://doi.org/10.1007/s00436-011-2577-z.
- Huff, C.G., 1957. Organ and tissue distribution of the exoerythrocytic stages of various avian malarial parasites. Exp. Parasitol. 6, 143–162. https://doi.org/ 10.1016/0014-4894(57)90012-7.
- Ilgūnas, M., Bukauskaitė, D., Palinauskas, V., Iezhova, T.A., Dinhopl, N., Nedorost, N., Weissenbacher-Lang, C., Weissenböck, H., Valkiūnas, G., 2016. Mortality and pathology in birds due to Plasmodium (Giovannolaia) homocircumflexum infection, with emphasis on the exoerythrocytic development of avian malaria parasites. Malar. J. 15, 256. https://doi.org/10.1186/s12936-016-1310-x.
- Ilgūnas, M., Bukauskaitė, D., Palinauskas, V., Iezhova, T., Fragner, K., Platonova, E., Weissenböck, H., Valkiūnas, G., 2019a. Patterns of *Plasmodium homocircumflexum* virulence in experimentally infected passerine birds. Malar. J. 18, 174. https://doi.org/10.1186/s12936-019-2810-2.
- Ilgūnas, M., Chagas, R.F., Bukauskaitė, C.D., Bernotienė, R., Iezhova, T., Valkiūnas, G., 2019b. The life-cycle of the avian haemosporidian parasite *Haemoproteus majoris*, with emphasis on the exoerythrocytic and sporogonic development. Parasit. Vectors 12, 516. https://doi.org/10.1186/s13071-019-3773-4.
- Ilgūnas, M., Himmel, T., Harl, J., Dagys, M., Valkiūnas, G., Weissenböck, H., 2022. Exo-erythrocytic development of avian haemosporidian parasites in European owls. Animals 12, 2212. https://doi.org/10.3390/ani12172212.
- Isobe, T., Akiba, K., 1990. Early schizonts of Leucocytozoon caulleryi. J. Parasitol. 76, 587. https://doi.org/10.2307/3282850.
- Jarvi, S.I., Schultz, J.J., Atkinson, C.T., 2002. PCR diagnostics underestimate the prevalence of avian malaria (Plasmodium relictum) in experimentally-infected passerines. J. Parasitol. 88, 153–158. https://doi.org/10.1645/0022-3395(2002) 088[0153:PDUTPO]2.0.CO;2.
- Knowles, S.C.L., Palinauskas, V., Sheldon, B.C., 2010. Chronic malaria infections increase family inequalities and reduce parental fitness: experimental evidence from a wild bird population. J. Evol. Biol. 23, 557–569.
- Križanauskienė, A., Hellgren, O., Kosarev, V., Sokolov, L., Bensch, S., Valkiūnas, G., 2006. Variation in host specificity between species of avian haemosporidian parasites: evidence from parasite morphology and cytochrome b gene sequences. J. Parasitol. 92, 1319–1324. https://doi.org/10.1645/GE-873R.1.
- la Puente, J.M., Merino, S., Tomás, G., Moreno, J., Morales, J., Lobato, E., García-Fraile, S., Belda, E.J., 2010. The blood parasite *Haemoproteus* reduces survival in a wild bird: a medication experiment. Biol. Lett. 6, 663–665. https://doi.org/10.1098/rsbl.2010.0046
- Lachish, S., Knowles, S.C.L., Alves, R., Wood, M.J., Sheldon, B.C., 2011. Fitness effects of endemic malaria infections in a wild bird population: the importance of ecological structure. Journal of Anim Ecol 80, 1196–1206. https://doi.org/ 10.1111/j.1365-2656.2011.01836.x.
- Lederer, R., Adlard, R.D., O'Donoghue, P.J., 2002. Severe pathology associated with protozoal schizonts in two pied currawongs (Strepera graculina) from Queensland. Vet. Rec. 150, 520–522. https://doi.org/10.1136/vr.150.16.520.
- Marinov, M.P., Marchetti, C., Dimitrov, D., Ilieva, M., Zehtindjiev, P., 2017. Mixed haemosporidian infections are associated with higher fearfulness in Yellow Wagtail (Motacilla flava). Can. J. Zool. 95, 405–410. https://doi.org/10.1139/cjz-2016-0121.
- Marzal, A., de Lope, F., Navarro, C., M
 øller, A.P., 2005. Malarial parasites decrease reproductive success: an experimental study in a passerine bird. Oecologia 142, 541–545. https://doi.org/10.1007/s00442-004-1757-2.
- Mata, V.A., da Silva, L.P., Lopes, R.J., Drovetski, S.V., 2015. The Strait of Gibraltar poses an effective barrier to host-specialised but not to host-generalised lineages of avian Haemosporidia. Int. J. Parasitol. 45, 711–719. https://doi.org/10.1016/j.ijpara.2015.04.006.
- Merino, S., Moreno, J., Sanz, J.J., Arriero, E., 2000. Are avian blood parasites pathogenic in the wild? A medication experiment in blue tits (Parus caeruleus). Proc. Biol. Sci. 267, 2507–2510. https://doi.org/10.1098/rspb.2000.1312.
- Morii, T., 1992. A review of *Leucocytozoon caulleryi* infection in chickens. J. Protozool. Res. 2, 128–133.
- Nakamura, K., 2022. *Leucocytozoon caulleryi* infection in chickens: etiology, pathology, and diagnosis. JARQ 56, 121–127. https://doi.org/10.6090/jarq.56.121.
- Niedringhaus, K.D., Fenton, H.M.A., Cleveland, C.A., Anderson, A.N., Schwartz, D., Alex, C.E., Rogers, K.H., Mete, A., Yabsley, M.J., 2018. Case series: virulent hemosporidiosis infections in juvenile great horned owls (Bubo virginianus) from Louisiana and California, USA. Vet Parasitol Reg Stud Rep 12, 49–54. https://doi.org/10.1016/j.vprsr.2018.01.008.
- Nilsson, E., Taubert, H., Hellgren, O., Huang, X., Palinauskas, V., Markovets, M.Y., Valkiūnas, G., Bensch, S., 2016. Multiple cryptic species of sympatric generalists within the avian blood parasite *Haemoproteus majoris*. J. Evol. Biol. 29, 1812–1826. https://doi.org/10.1111/jeb.12911.
- Ortiz-Catedral, L., Brunton, D., Stidworthy, M.F., Elsheikha, H.M., Pennycott, T., Schulze, C., Braun, M., Wink, M., Gerlach, H., Pendl, H., Gruber, A.D., Ewen, J., Pérez-Tris, J., Valkiūnas, G., Olias, P., 2019. *Haemoproteus minutus* is highly virulent for Australasian and South American parrots. Parasit. Vectors 12, 40. https://doi.org/10.1186/s13071-018-3255-0.
- Pacheco, M.A., Matta, N.E., Valkiūnas, G., Parker, P.G., Mello, B., Stanley, C.E., Lentino, M., Garcia-Amado, M.A., Cranfield, M., Kosakovsky Pond, S.L., Escalante, A.A., 2018. Mode and rate of evolution of haemosporidian mitochondrial genomes: timing the radiation of avian parasites. Mol. Biol. Evol. 35, 383–403. https://doi.org/10.1093/molbey/msx285.
- Palinauskas, V., Valkiūnas, G., Bolshakov, C.V., Bensch, S., 2008. Plasmodium relictum (lineage P-SGS1): effects on experimentally infected passerine birds. Exp. Parasitol. 120, 372–380. https://doi.org/10.1016/j.exppara.2008.09.001.

- Palinauskas, V., Valkiūnas, G., Križanauskienė, A., Bensch, S., Bolshakov, C.V., 2009. Plasmodium relictum (lineage P-SCS1): Further observation of effects on experimentally infected passeriform birds, with remarks on treatment with Malarone. Exp. Parasitol. 123, 134–139. https://doi.org/10.1016/ j.exppara.2009.06.012.
- Paperna, I., Gill, H., 2003. Schizogonic stages of *Haemoproteus* from Wenyon's Baghdad sparrows are also found in Passer domesticus biblicus in Israel. Parasitol. Res. 91, 486–490. https://doi.org/10.1007/s00436-003-0967-6.
- Peirce, M.A., 1976. Haemoproteid parasites of *Passer* spp. Parasitology 73, 407–415. https://doi.org/10.1017/S0031182000047077.
- Peirce, M.A., 1981. Distribution and host-parasite check-list of the haematozoa of birds in western europe. J. Nat. Hist. 15, 419–458. https://doi.org/10.1080/00222938100770321.
- Peirce, M.A., Lederer, R., Adlard, R.D., O'Donoghue, P.J., 2004. Pathology associated with endogenous development of haematozoa in birds from southeast Queensland. Avian Pathol. 33, 445–450. https://doi.org/10.1080/03079450410001724076.
- Pellegrino, I., Ilahiane, L., Boano, G., Cucco, M., Pavia, M., Prestridge, H.L., Voelker, G., 2021. Avian haemosporidian diversity on Sardinia: a first general assessment for the insular mediterranean. Diversity (Basel) 13, 75. https://doi.org/10.3390/ d13020075.
- Pendl, H., Hernández-Lara, C., Kubacki, J., Borel, N., Albini, S., Valkiūnas, G., 2022. Exo-erythrocytic development of Plasmodium matutinum (lineage pLINN1) in a naturally infected roadkill fieldfare Turdus pilaris. Malar. J. 21, 148. https://doi.org/10.1186/s12936-022-04166-x.
- Pennycott, T., Wood, A., MacIntyre, C., MacIntyre, D., Patterson, T., 2006. Deaths in aviary birds associated with protozoal megaloschizonts. Vet. Rec. 159, 499–500. https://doi.org/10.1136/vr.159.15.499.
- Pérez-Tris, J., Bensch, S., 2005. Diagnosing genetically diverse avian malarial infections using mixed-sequence analysis and TA-cloning. Parasitology 131, 15–23. https://doi.org/10.1017/S003118200500733X.
- Pohuang, T., Jittimanee, S., Junnu, S., 2021. Pathology and molecular characterization of *Leucocytozoon caulleryi* from backyard chickens in Khon Kaen Province, Thailand. Vet World 14, 2634–2639. https://doi.org/10.14202/vetworld.2021.2634-2639.
- Ronquist, F., Teslenko, M., Van Der Mark, P., Ayres, D.L., Darling, A., Höhna, S., Larget, B., Liu, L., Suchard, M.A., Huelsenbeck, J.P., 2012. Mrbayes 3.2: efficient bayesian phylogenetic inference and model choice across a large model space. Syst. Biol. 61, 539–542. https://doi.org/10.1093/sysbio/sys029.
- Ross, J.M., Kim, C., Allen, D., Crouch, E.E., Narsinh, K., Cooke, D.L., Abla, A.A., Nowakowski, T.J., Winkler, E.A., 2020. The expanding cell diversity of the brain vasculature. Front. Physiol. 11, 1–13. https://doi.org/10.3389/fphys.2020.600767.
- Rozas, J., Ferrer-Mata, A., Sánchez-DelBarrio, J.C., Guirao-Rico, S., Librado, P., Ramos-Onsins, S.E., Sánchez-Gracia, A., 2017. DnaSP 6: DNA sequence polymorphism analysis of large data sets. Mol. Biol. Evol. 34, 3299–3302. https://doi.org/10.1093/molbev/msx248.
- Santiago-Alarcon, D., Palinauskas, V., Schaefer, H.M., 2012. Diptera vectors of avian Haemosporidian parasites: untangling parasite life cycles and their taxonomy. Biol. Rev. 87, 928–964.
- Santiago-Alarcon, D., MacGregor-Fors, I., Kühnert, K., Segelbacher, G., Schaefer, H.M., 2016. Avian haemosporidian parasites in an urban forest and their relationship to bird size and abundance. Urban Ecosyst. 19, 331–346. https://doi.org/ 10.1007/s11252-015-0494-0.
- Sawale, G.K., Dhaygude, V.S., Moregaonkar, S.D., 2018. Outbreak of leucocytozoonosis in layer birds. Indian Vet. J. 95, 42–44.
- Scheuerlein, A., Ricklefs, R.E., 2004. Prevalence of blood parasites in European passeriform birds. Proc. Biol. Sci. 271, 1363–1370. https://doi.org/10.1098/rspb.2004.2726.
- Schindelin, J., Arganda-Carreras, I., Frise, E., Kaynig, V., Longair, M., Pietzsch, T., Preibisch, S., Rueden, C., Saalfeld, S., Schmid, B., Tinevez, J.Y., White, D.J., Hartenstein, V., Eliceiri, K., Tomancak, P., Cardona, A., 2012. Fiji: an open-source platform for biological-image analysis. Nat. Methods 9, 676–682. https://doi.org/10.1038/nmeth.
- Sibley, L.D., Werner, J.K., 1984. Susceptibility of pekin and muscovy ducks to Haemoproteus nettionis. J. Wildl. Dis. 20, 108–113. https://doi.org/10.7589/ 0090-3558-20.2.108.
- Skalli, O., Pelte, M.F., Peclet, M.C., Gabbiani, G., Gugliotta, P., Bussolati, G., Ravazzola, M., Orci, L., 1989. α-Smooth muscle actin, a differentiation marker of smooth muscle cells, is present in microfilamentous bundles of pericytes. J. Histochem. Cytochem. 37, 315–321. https://doi.org/10.1177/37.3.2918221.
- Smith, A.F., Doyeux, V., Berg, M., Peyrounette, M., Haft-Javaherian, M., Larue, A.-E., Slater, J.H., Lauwers, F., Blinder, P., Tsai, P., Kleinfeld, D., Schaffer, C.B., Nishimura, N., Davit, Y., Lorthois, S., 2019. Brain capillary networks across species: a few simple organizational requirements are sufficient to reproduce both structure and function. Front. Physiol. 10, 1–22. https://doi.org/10.3389/fphys.2019.00233.
- Stidworthy, M.F., Greenwood, A.G., 2006. Deaths in aviary birds associated with protozoal megaloschizonts. Vet. Rec. 159, 606. https://doi.org/10.1136/vr.159.18.606.
- Striepen, B., Jordan, C.N., Reiff, S., van Dooren, G.G., 2007. Building the perfect parasite: cell division in Apicomplexa. PLoS Pathog. 3, e78.
- Trifinopoulos, J., Nguyen, L.-T., von Haeseler, A., Minh, B.Q., 2016. W-IQ-TREE: a fast online phylogenetic tool for maximum likelihood analysis. Nucleic Acids Res. 44, W232–W235. https://doi.org/10.1093/nar/gkw256.

- Valkiūnas, G., 2005. Avian Malaria Parasites and other Haemosporidia. CRC Press, Boca Raton.
- Valkiūnas, G., lezhova, T.A., 2017. Exo-erythrocytic development of avian malaria and related haemosporidian parasites. Malar. J. 16, 101. https://doi.org/10.1186/s12936-017-1746-7.
- Valkiūnas, G., lezhova, T.A., 2018. Keys to the avian malaria parasites. Malar. J. 17, 212. https://doi.org/10.1186/s12936-018-2359-5.
- Valkiūnas, G., lezhova, T.A., 2022. Keys to the avian Haemoproteus parasites (Haemosporida, Haemoproteidae). Malar. J. 21, 269. https://doi.org/10.1186/s12936-022-04235-1.
- Valkiūnas, G., Iezhova, T.A., Shapoval, A.P., 2003. High prevalence of blood parasites in hawfinch *Coccothraustes coccothraustes*. J. Nat. Hist. 37, 2647–2652. https://doi.org/10.1080/002229302100001033221.
- Valkiūnas, G., Bensch, S., Iezhova, T.A., Križanauskienė, A., Hellgren, O., Bolshakov, C. V., 2006. Nested cytochrome b polymerase chain reaction diagnostics

- underestimate mixed infections of avian blood haemosporidian parasites: microscopy is still essential. J. Parasitol. 92, 418–422. https://doi.org/10.1645/GE-3547RN.1.
- Valkiūnas, G., Iezhova, T.A., 2023. Insights into the biology of Leucocytozoon species (Haemosporida, Leucocytozoidae): why is there slow research progress on agents of leucocytozoonosis? Microorganisms 11, 1251. https://doi.org/10.3390/microorganisms11051251.
- van Rooyen, J., Lalubin, F., Glaizot, O., Christe, P., 2013. Avian haemosporidian persistence and co-infection in great tits at the individual level. Malar. J. 12, 40. https://doi.org/10.1186/1475-2875-12-40.
- Yablonka-Reuveni, Z., 1989. The emergence of the endothelial cell lineage in the chick embryo can be detected by uptake of acetylated low density lipoprotein and the presence of a von Willebrand-like factor. Dev. Biol. 132, 230–240. https://doi.org/10.1016/0012-1606(89)90219-4.